



The *FpPPR1* Gene Encodes a Pentatricopeptide Repeat Protein That Is Essential for Asexual Development, Sporulation, and Pathogenesis in *Fusarium pseudograminearum*

OPEN ACCESS

Edited by:

Qinhu Wang,
Northwest A and F University, China

Reviewed by:

Changjun Chen,
Nanjing Agricultural University, China
Rahim Mehrabi,
Isfahan University of Technology, Iran

*Correspondence:

Shengli Ding
shengli ding@henau.edu.cn
Shen Liang
liangshen1@126.com
Honglian Li
honglianli@sina.com

Specialty section:

This article was submitted to
Evolutionary and Genomic
Microbiology,
a section of the journal
Frontiers in Genetics

Received: 17 February 2020

Accepted: 09 December 2020

Published: 15 January 2021

Citation:

Wang L, Xie S, Zhang Y, Kang R, Zhang M, Wang M, Li H, Chen L, Yuan H, Ding S, Liang S and Li H (2021) The *FpPPR1* Gene Encodes a Pentatricopeptide Repeat Protein That Is Essential for Asexual Development, Sporulation, and Pathogenesis in *Fusarium pseudograminearum*. *Front. Genet.* 11:535622. doi: 10.3389/fgene.2020.535622

Limin Wang¹, Shunpei Xie¹, Yinshan Zhang¹, Ruijiao Kang^{1,2}, Mengjuan Zhang¹, Min Wang¹, Haiyang Li¹, Linlin Chen¹, Hongxia Yuan¹, Shengli Ding^{1*}, Shen Liang^{3*} and Honglian Li^{1*}

¹ Henan Agricultural University/Collaborative Innovation Center of Henan Grain Crops/National Key Laboratory of Wheat and Maize Crop Science, Zhengzhou, China, ² Xuchang Vocational Technical College, Xuchang, China, ³ Horticulture Research Institute, Henan Academy of Agricultural Sciences, Zhengzhou, China

Fusarium crown rot (FCR) and *Fusarium* head blight (FHB) are caused by *Fusarium pseudograminearum* and are newly emerging diseases of wheat in China. In this study, we characterized *FpPPR1*, a gene that encodes a protein with 12 pentatricopeptide repeat (PPR) motifs. The radial growth rate of the $\Delta Fppr1$ deletion mutant was significantly slower than the wild type strain WZ-8A on potato dextrose agar plates and exhibited significantly smaller colonies with sector mutations. The aerial mycelium of the mutant was almost absent in culture tubes. The $\Delta Fppr1$ mutant was able to produce spores, but spores of abnormal size and altered conidium septum shape were produced with a significant reduction in sporulation compared to wild type. $\Delta Fppr1$ failed to cause disease on wheat coleoptiles and barley leaves using mycelia plugs or spore suspensions. The mutant phenotypes were successfully restored to the wild type levels in complemented strains. FpPpr1-GFP signals in spores and mycelia predominantly overlapped with Mito-tracker signals, which substantiated the mitochondria targeting signal prediction of FpPpr1. RNAseq revealed significant transcriptional changes in the $\Delta Fppr1$ mutant with 1,367 genes down-regulated and 1,333 genes up-regulated. NAD-binding proteins, thioredoxin, 2Fe-2S iron-sulfur cluster binding domain proteins, and cytochrome P450 genes were significantly down-regulated in $\Delta Fppr1$, implying the dysfunction of mitochondria-mediated reductase redox stress in the mutant. The mating type idiomorphic alleles *MAT1-1-1*, *MAT1-1-2*, and *MAT1-1-3* in *F. pseudograminearum* were also down-regulated after deletion of *FpPPR1* and validated by real-time quantitative PCR. Additionally, 21 genes encoding putative heterokaryon incompatibility proteins were down-regulated. The yellow pigmentation of

the mutant was correlated with reduced expression of *PKS12* cluster genes. Taken together, our findings on *FpPpr1* indicate that this PPR protein has multiple functions in fungal asexual development, regulation of heterokaryon formation, mating-type, and pathogenesis in *F. pseudograminearum*.

Keywords: *Fusarium pseudograminearum*, pentatricopeptide repeat, *FpPPR1*, mitochondrial, pathogenesis, wheat, aerial hyphae

INTRODUCTION

The winter wheat region in Huang Huai plain is the main wheat production area in China. Within this region, the Henan Province has the highest planting area and yield. A winter wheat-summer corn double cropping system has been the main manner of tillage in this region for many years. Wheat stubble on the soil surface or buried stubble are retained in this region to promote soil structure and nutrition (Zhang et al., 2007), however, this practice also allows for the accumulation of soil-borne fungal pathogens (Burgess et al., 1996). In recent years, *Fusarium* crown rot (FCR), mostly caused by soil-borne fungal pathogens *F. pseudograminearum*, *F. graminearum*, and *F. culmorum*, became an emerging disease in the Huang Huai winter region, leading to losses in yield (Zhou et al., 2014; Li et al., 2016). In the pathogen complex, *F. pseudograminearum* was predominant and had been detected in seven provinces (Zhou et al., 2019; Deng et al., 2020). FCR is a common disease of wheat and barley worldwide with typical symptoms of brown discoloration on the crown, leaf sheathes, lower stem tissues, and white heads (Smiley et al., 2005). Infected wheat by *F. pseudograminearum* might reduce kernel weight, numbers of kernels per head, grain weight, tiller height, and straw weight (Smiley et al., 2005). In Henan, the FCR caused 38.0 to 61.3% in yield losses from 2013 to 2016 (Xu et al., 2016). In Australia, nearly AU \$80 million was lost annually due to FCR (Murray and Brennan, 2009). In the United States, FCR reduced winter wheat yields 9.5 to 35% in the commercial fields from 1993 to 2001 (Smiley et al., 2005).

Fusarium head blight (FHB), predominantly caused by *F. graminearum* in Huang Huai winter wheat region, was also detected by *F. pseudograminearum* in three provinces Henan, Hebei, and Shandong (Ji et al., 2015; Xu et al., 2015), which had led to epidemics in Australia (Burgess et al., 1987; Miedaner et al., 2010; Obanor et al., 2013; Kazan and Gardiner, 2017). In Henan, Li et al. (2017) isolated pathogens from 250 of the diseased wheat head samples in the fields and the detection rates for *F. graminearum* and *F. pseudograminearum* were 83.3 and 55.6%, respectively. *F. pseudograminearum* can survive in stubble residues for up to three years, thereby increasing the amount of inoculum (Summerell and Burgess, 1988; Dodman and Wildermuth, 1989; Backhouse, 2014).

The screening of 88 local wheat cultivars-caused by *F. pseudograminearum* under artificial inoculation assay was conducted and showed that 88.64% (78/88) of the current varieties of wheat were susceptible or highly susceptible to FCR, while the remaining 10 cultivars exhibited moderate resistance at the adult stage (Yang et al., 2015). The mechanism of resistance to FCR remains obscure. Even some QTLs were

identified for adult plant with partial resistance to crown rot by *F. pseudograminearum* in the bread wheat (Bovill et al., 2010), the low resolution of genetic mapping of major QTLs for the resistance of FCR is a major hurdle in wheat plant breeding (Liu et al., 2015).

Fusarium pseudograminearum is a hemibiotrophic fungus but the molecular mechanism involved in its pathogenesis has not been revealed. The entire genomes of *F. pseudograminearum* for the initial *MAT1-1* strain CS3096, the *MAT1-1* strain CS3270, along with the *MAT1-2* strain RGB5226 have been subsequently sequenced (Gardiner et al., 2012, 2016). In a comparative genomic analysis, Gardiner et al. (2012) identified the horizontal movement of the *FaAH1* gene from a bacterium and the *DLH1-AMD1* two-gene cluster. *FpAH1* and *FpDLH1* encode a putative amidohydrolase and a putative dienelactone hydrolase, respectively, contributing to the virulence of barley or wheat, while *FpAH1* appears to have a host-specific selection between barley and wheat. Wheat produces defense compounds such as the benzoxazolin class of phytoalexins 6-netgixt-benzoxazolin-2-one (MBOA) and benzoxazolin-2-one (BOA) (Villagrasa et al., 2006; Powell et al., 2017). The *Fusarium* Detoxification of Benzoxazolinone (FDB) gene cluster including *FDB1*, *FDB2*, and *FDB3* encoding a γ -lactamase, N-malonyltransferase, and GAL4-like Zn (II)₂Cys₆ transcription factor, respectively, are involved in BOA and MBOA detoxification in wheat (Gardiner et al., 2012; Kettle et al., 2015a,b, 2016).

The whole genome sequencing promotes virulence genes characterization in the pathogenesis. Wang L. M. et al. (2017) found that *FpPDE1* encodes a putative P-type ATPase that is required for full virulence on wheat and barley. Chen et al. (2018) reported that 26 genes out of 29 autophagy-related (ATGs) genes were induced with differential expression levels during early or late stages of wheat infection. *FpLhs1*, one of 14 Hsp70 proteins, regulated fungal development, asexual reproduction, and pathogenicity through the protein secretion pathway (Chen et al., 2019a). The basic leucine zipper (bZIP) *FpAda1*, was essential for vegetative growth, conidiation, and full virulence of wheat seedling hypocotyls and root growth. The expressions of *FpCdc42* and *FpCdc2* during cell cycle regulation were regulated by *FpAda1* (Chen et al., 2019b). The eleven genes encoding putative basic helix-loop-helix (bHLH) transcriptional regulators were differentially expressed during infection of wheat and three bHLH genes were induced during infection and contributed to virulence in wheat (Chen et al., 2019c).

To investigate secondary metabolism in this fungus, Kang et al. (2020) characterized a nonribosomal peptide gene, *FpNPS9*, where the deletion mutant showed normal colony morphology, growth rate, and conidiation, but infection was strongly restricted

in wheat coleoptiles and heads, indicating an interaction with the endogenous defense systems of wheat. DON production was also down-regulated in the *FpNPS9* mutant. Zhang et al. (2020) investigated *FpDEP1*, a yeast DEP1 ortholog, which was found to be involved in Rpd3L complex regulation of pleiotropic functions, including vegetative growth, conidiation, pathogenicity, inhibition of host defense, reactive oxygen species (ROS) accumulation, and vacuole membrane biogenesis.

Pentatricopeptide repeat (PPR) proteins usually consist of arrays of a degenerate 35 amino-acid structural motif and are usually present in organelles of eukaryotic cells (Small and Peeters, 2000). There are 450 plus PPR members in higher land plants and fewer numbers in fungi and mammals (Lurin et al., 2004; Schmitz-Linneweber and Small, 2008). PPR proteins play important roles in growth and development in plants (Wang et al., 2018). Physiological effects on oxidative phosphorylation in defective PPR proteins can cause human diseases (Lightowers and Chrzanoska-Lightowers, 2008). The budding yeasts, *Saccharomyces cerevisiae* and *S. pombe*, and humans have only 15, 10, and 7 PPR proteins, respectively (Herbert et al., 2013). A PPR protein *ppr10* in *S. pombe* functions as a general translational activator, which is stabilized by *Mpa1*. The deletion of *ppr10* affects the accumulation of specific mitochondrial mRNAs (Wang Y. et al., 2017). Loss of *ppr3*, *ppr4*, *ppr6*, or *ppr10* leads to non-sexual flocculation and filamentous growth of cells (Su et al., 2017, 2018). In filamentous fungi, nine PPR genes were found in *Neurospora crassa* and four of them were functionally characterized, including one that encodes Cya-5 (Cytochrome *c* oxidase) which is involved in post-transcriptional processing. Both Cya-5 in *N. crassa* and PET309 in *Saccharomyces cerevisiae*, partial ortholog of PPR proteins, regulate *COXI* (Cytochrome *c* oxidase, aa3 type, subunit I) translation and stability. *COXI* expression is required for the synthesis of respiratory complex I and targeted RNA processes in mitochondria, but it is not clear whether the assembly factor CIA84 (complex I intermediate associated proteins is involved) is involved in RNA editing (Coffin et al., 1997; Moseler et al., 2012). The objective of this study was to identify the pentatricopeptide repeat (PPR) gene in *F. pseudograminearum* and to reveal the function of PPR gene in the filamentous phytopathogen.

MATERIALS AND METHODS

Sequence Analysis

Sequences were analyzed using DNASTAR software (Bioinformatics Software for Life Science-DNASTAR)¹, BLASTn, or BLASTp (Nucleotide BLAST on National Center for Biotechnology Information)², and local BLAST against the genome of *Fusarium oxysporum* f. sp. *lycopersici* 4287 and *F. pseudograminearum* CS3096³. The predicted protein PPR domains were analyzed by TPRpred in the MPI Bioinformatics

Toolkit⁴. SMART analysis from the Pfam database with amino acid residues predicted the domains⁵. Alignment of amino acid sequences and phylogenetic analysis were performed using DNAMAN and MEGA6 software, respectively.

Fungal Strains and Culture Conditions

The *F. pseudograminearum* strain used in this study was the local isolate WZ-8A reserved at Henan Agricultural University. Solid potato dextrose agar (PDA; 200 g peeled potato, 20 g dextrose, 15 g agar, and 1 L water), liquid Yeast Peptone Glucose media (YPG; 1% yeast extract, 2% peptone, and 2% dextrose), and sporulation media consisting of carboxymethyl cellulose liquid media (CMC; 2% solution of CMC) preparations as well as the culture conditions were adopted from a previous report (Wang L. M. et al., 2017).

Gene Deletion and Complementation in *F. pseudograminearum*

The split-marker strategy was applied to delete the candidate gene following Catlett et al. (2003). The detailed approach for gene deletion in *F. pseudograminearum* was further described by Wang L. M. et al. (2017). Briefly, the amplification of upstream, downstream, and hygromycin fragment were amplified (The primers used in this study are listed in **Supplementary Table 1**). A mixture of upstream and downstream with hygromycin fusion fragments, D1H1 and D2H2, generated from recombinant fusion fragment D1-H-D2 (**Figures 2A,B**), were used for the transformation of protoplasts of *F. pseudograminearum* wild type WZ-8A. PCR screening of putative knockouts and further Southern blot analysis were performed (**Figure 2C**).

To recover the defects deletion mutant, a fusion construct pFpPPR1-GFP with 1.6-kb native promoter was generated and transformed into protoplasts of the $\Delta Fpppr1$ deletion mutant. The GFP signal of the complemented transformants from conidia, germ tubes, and mycelia of candidates was checked with a Nikon fluorescent Eclipse inverted Ti-S microscope. The colony morphology, radial growth, conidiation, and pathogenicity were then evaluated.

Biological Assays

A 5 mm plug was placed on a 9-cm Petri dish containing 15 mL of PDA medium. Colony diameter was measured after a 3 d incubation at 25°C for the *FpPPR1* deletion mutant, complemented strain, and the wild type WZ-8A. The measurement for each colony was recorded on a perpendicular plane, giving an average value. Each strain was subjected to three independent experiments with at least three plates each. The statistical analysis of our results was performed via Student's *t*-test in Excel worksheet.

To test sporulation, 7 mm fungal mycelia blocks were put in a 250 mL flask containing 100 mL CMC media with shaking at 150 rpm for 5 d at 25°C. All tests had three replicates. Spore morphology and their germination were observed under a microscope. The spores at 1×10^5 /mL were dropped onto sterile

¹www.dnastar.com

²https://www.ncbi.nlm.nih.gov/

³http://fungi.ensembl.org/

⁴https://toolkit.tuebingen.mpg.de/#/tools/psiblast

⁵http://smart.embl-heidelberg.de

glass slides. The slides were placed in a moist plastic container kept at 25°C. The spore germination rate was counted using at least 200 conidia with three repeats.

To determinate the defects of the mutants on reactive oxidative stress *in vivo*, the toleration to H₂O₂ was assayed on the solid medium plate containing 10 mM H₂O₂. For analysis of the response to different wall or membrane stresses, Congo red and sodium dodecyl sulfate (SDS) was supplemented in the culture medium containing 0.2 g/L Congo red or 0.05% (w/v) SDS. All the test of sensitivities to several stresses were carried out on 70-mm PDA plates at 25°C for 3 d. The perpendicular cross measurements method was applied to measure the colony diameter. The inhibition rate was calculated by formula inhibition rate = $[(C-N)/(C-5)] \times 100$, where C is the colony diameter of the control and N is the colony diameter of the treatment (Chen et al., 2019).

Pathogenicity Test

To determine pathogenicity, the seeds of the susceptible wheat cultivar Aikang58 were treated with 3% sodium hypochlorite solution for 3 min for sterilization, followed by three times washes with sterile water. After incubation in 10 cm diameter plates to accelerate germination, seedlings with shoots were placed on wet filter paper in a tray. The coleoptiles around 3 cm high were inoculated with 5-mm fungal block taken from 3 d old PDA cultures. The test had three replicates with 4-5 coleoptiles each. After 24 h of dark incubation at 25°C, fungal blocks were removed, and wheat plants were placed in a greenhouse at 25°C (47% humidity) with a 16 h light/8 h dark photoperiod. After 3 d incubation, the plants were photographed.

Spore suspensions at 10⁶/mL or 5-mm fungal plugs from PDA plates after 3 d incubation at 25°C were inoculated on barley leaves for evaluation of the pathogenicity of *F. pseudograminearum* as described by Zhang et al. (2020). After treatment of 3% sodium hypochlorite (NaOCl) solution for 3 min, seeds of barley cultivar Kenpimai 13 (generously provided by Baocang Ren, Research Associate, from Gansu Academy of Agricultural Sciences) was washed twice with sterile water and submerged in distilled water for 24 h in a beaker at 25°C. The imbibed seeds were placed into a plastic tray filled with a turfy soil mix (pH 5.5–7.0, humic acid $\geq 5.0\%$, organic substrate $\geq 25.0\%$, Shouguang Wode Agricultura Technology Co. LTD, Shandong, China). After planting, the tray was covered with plastic foil and put into a humid chamber (25°C, 16 h photoperiod, 47% humidity) for 5–7 d. The plastic foil was removed when the shoot reached 1 cm in height. Five to six barley seedlings (one formed leaf stage) were taken out of soil mix, laid horizontally in a new tray with the roots wrapped in a moist paper towel and leaves fixed on the surface of the tray by tape. Each treatment contained 5–6 leaves in a tray.

Mitochondria Staining

Five to eight 7-mm fungal plugs from the leading edge of a 3-d-old colony of the complemented strain (cFppr1) on PDA were transferred into a 250 mL flask containing 100 mL of CMC liquid media with shaking at 150 rpm at 25°C for 4–5 d. The conidia were harvested into a 50 mL microcentrifuge tube after filtering

through one-layer sterile Miracloth. The conidia suspension was centrifuged at 2,500 g and supernatant was removed then resuspended in 1 mL of Phosphate buffered saline (PBS) and centrifuged again. After the second wash, 1×10^5 conidia in a fresh tube were resuspended in prewarmed Mito-Tracker Red CMXRos M7512 at 37°C (MitoTracker mitochondrion-selective probes, Invitrogen) working solution (200 nM in PBS from the stock solution at –20°C, protected from light) for 10 min of staining following the kit instruction. The conidia were pelleted at 5,000 g for 3 min and resuspended in 50 μ L of PBS for imaging with fluorescent GFPHQ green and TRITC red filters with a Nikon fluorescence Eclipse inverted Ti-S microscope.

DNA Extraction and Southern Blot

Mycelia preparation for genomic DNA extraction and Southern blotting followed the previous method reported by Wang L. M. et al. (2017). The genomic DNA was extracted with the CTAB (2% CTAB (cetyl trimethyl ammonium bromide), 20 mM EDTA, 0.1 M Tris-HCl, and 1.4 M NaCl, plus 2% (v/v) 2-Mercaptoethanol added just before use) method (Lee et al., 1988). About 10 μ g DNA of each strain was digested by *Xho* I, respectively, separated within a 0.8% agarose gel, blotted to Hybond N + membrane (GE Healthcare Life Sciences, United States), and detected following manufacturer's instruction (Roche Diagnostics, United States) with *FpPPR1* fragment as probe 1 and the hygromycin resistance gene fragment as probe 2 labeled with Roche's DIG High Prime DNA Labeling and Detection Kit II according to the manufacturer's instructions.

RNA-Seq Analysis

The wild type WZ-8A and mutant strains transferred to PDA plates from –80°C stock were incubated at 25°C for 3 d. A 1 cm square of the PDA culture block was cut and put into a blender (Weike ZW800D, Wenzhou Weike Biology Experiment Equipment Co., LTD) containing 100 mL of YPG liquid medium for 5 s of homogenization at 4,000 rpm/min. The homogenates were transferred into 250 mL flasks for mycelia growth rotating at 150 rpm/min at 25°C. After 3 d of growth, the mycelia were harvested by filtering through sterile Miracloth into a funnel (475855-R, EMD Millipore Corp)⁶ and rinsing mycelia twice with sterile distilled water.

For RNA-seq, three biological mycelia samples derived from wild type WZ-8A and the $\Delta Fppr1$ deletion mutant were sent to Seqhealth Technology Co., LTD (Wuhan, China) for RNA extraction using TRIzol Reagent (Invitrogen, cat. NO 15596026) following the provided instructions. cDNA libraries were constructed using the KC-Digital™ Stranded mRNA Library Prep Kit for Illumina® (Catalog NO. DR08502, Wuhan Seqhealth Co., Ltd. China) following the manufacturer's instruction. The library products around 200–500 bp in length were sequenced on a Novaseq 6000 sequencer (Illumina; PE150 model). The clean reads were mapped to the reference genome of *F. pseudograminearum* CS3096 (Gardiner et al., 2012)⁷ using the STAR software (version 2.5.3a) with default parameters.

⁶www.millipore.com

⁷https://mycoscosm.jgi.doe.gov/Fusps1/Fusps1.home.html

The mapped read counts were converted to RPKM (Reads per Kilobase per Million Reads). Genes differentially expressed between samples were identified using the edgeR package (version 3.12.1) (Robinson et al., 2010; McCarthy et al., 2012). The differentially expressed genes (DEGs) were defined via fold change (FC) in $\log_2(\text{FC})$ greater than 1.0 as calculated by the RPKM value of the same gene between mutant and wild type with the thresholds of both the *p*-value and the corrected *p*-value <0.05 to avoid false positives. Gene ontology (GO) analysis and Kyoto encyclopedia of genes and genomes (KEGG) enrichment analysis for differentially expressed genes were both implemented by KOBAS software (version: 2.1.1) with a *p*-value cutoff of 0.05 to assess statistically significant enrichment.

Real-Time Quantitative PCR

For quantitative assays, the total RNA of wild type WZ-8A and $\Delta Fpppr1$ deletion mutant was extracted using the Trizol reagent (Ambion by Life Technologies 15596026) following the manufacturer's instructions. The integrity of RNA quality was assessed by agarose gel electrophoresis and measured using an ultramicro spectrophotometer (Thermo). cDNA was synthesized according to the manual instructions of the PrimeScript® RT reagent Kit (Perfect Real Time, TaKaRa Code: DRR047A). Briefly, the first strand cDNAs derived from 1 μg total RNA after removing the genomic DNA were synthesized in a 20 μL mix using an RT-PCR kit (PrimeScript RT reagent kit with gDNA eraser, code No. RR047A, TaKaRa) following the instructions. The 100 ng cDNA was used as the template in a 20 μL mix for qPCR using TB Green Premi Ex Taq II (Tli RNaseH Plus, Code No. RR820Q; TaKaRa). The cycling conditions were as follows: pre-denaturation at 95°C for 2 min followed by 40 cycles of denaturation at 95°C for 15s, annealing at 58°C for 15 s, extension at 68°C for 20 s, and a final stage at 95°C for 15 s to generate a melting curve. The RT-PCR was performed on Eppendorf realplex4 with software realplex Nr:6302 900 220-14. The quantitative results were calculated and analyzed using the $2^{-\Delta\Delta C_t}$ method with normalization to the CT value of an actin gene (Livak and Schmittgen, 2001). The gene candidates were selected to validate the RNA-seq results. The primers used in the test were listed in **Table 1**.

RESULTS

Identification of *FpPPR1* in *F. pseudograminearum*

From a screen of a T-DNA insertion library of *F. oxysporum* f. sp. *niveum* (FON) strain FON-11-06, we identified the FOXG_08514 gene in *Fusarium oxysporum* f. sp. *lycopersici* 4287 as a pentatricopeptide (PPR)-containing protein. The disrupted mutant exhibited a significantly reduced radial growth, less purple pigment on colony, and lost pathogenicity on watermelon seedlings. We continued to investigate its orthologue in *F. pseudograminearum* with significance in wheat production of Huanghuai winter regions.

Local BLASTp against the *F. pseudograminearum* genome database using the FOXG_08514 amino acid sequence revealed

the ortholog gene FPSE_02553 (**Supplementary Document**). We analyzed FPSE_02553 using the *F. pseudograminearum* genome database⁸ and transcriptome data for the local strain WZ-8A. The FPSE_02553 locus was on the third chromosome with a predicted cDNA of 3,624 bp and a predicted protein of 1,207 amino acid residues without introns. SMART analysis (Pfam) of the FPSE_02553 amino acid residues predicted PPR domains in 3 particular positions (**Figure 1A**)⁹. BLASTp analysis against UniProtKB determined the identities of the translated protein *cya5* in *Fusarium langsethiae* and *F. oxysporum* from orthologs to *cya5* at a range of 58.1 to 87.1% identities in *F. langsethiae*, *F. oxysporum*, *F. proliferatum*, *F. mangiferae*, and *Gibberella fujikuroi*, as well as the PPR proteins at 41.2 to 42.1% identities in *Tolypocladium ophioglossoides*, *T. paradoxum*, *Hypocrea jecorina*, *T. capitatum*, and *Escovopsis weberi*. The translated protein *cya5* is also a PPR-containing protein. A phylogenetic tree was constructed based on the alignment of amino acids (**Figure 1B**). The 7 PPR-repeat conserved domains from BLAST results were listed. Further prediction through TPRpred in the MPI Bioinformatics Toolkit identified 12 putative PPR motifs consisting of 35 degenerate amino acids (**Figures 1C,D**)¹⁰. Therefore, we designated FPSE_02553 as an *F. pseudograminearum* PPR gene, *FpPPR1*.

Knockout of *FpPPR1*

To determine the function of *FpPPR1* in *F. pseudograminearum*, we used a split-marker strategy to obtain hygromycin-resistant knockout transformants. After PCR screening with negative and positive primer pairs, three candidates were used for further Southern blot analysis. When hybridized with the hygromycin gene as a probe, $\Delta Fpppr1-3$ and $\Delta Fpppr1-4$ had a 2.9-kb band, but $\Delta Fpppr1-4$ with one extra insertion event. $\Delta Fpppr1-3$ strain was no band detected (wild type had a band of 5.2 kb) when hybridized with the *FpPPR1* fragment as a probe, which suggested that $\Delta Fpppr1-3$ was the clean knockout mutant (**Figure 2C**). The $\Delta Fpppr1-3$ strain would be used as the $\Delta Fpppr1$ mutant in the following assays.

The band of 2.9-kb *Xho* I indicates the target gene replacement, while one extra band suggests that the single copy insertion event occurred after the homologue replacement from two fragments of hygromycin gene. At the meantime, the random insertion of the fused hygromycin gene with function in the genome, might potentially display a side effects besides the target gene deletion. The $\Delta Fpppr1-5$ line was just an ectopic insertion strain without the target gene replacement events (**Figure 2C**), where the fused fragment including hygromycin gene was inserted in the genome randomly.

$\Delta Fpppr1$ Exhibits Deficient Vegetative Growth, Weaken Conidiation, and Altered Conidia Morphology

Colonies of the $\Delta Fpppr1$ mutant on PDA plates were significantly smaller ($p < 0.01$) than those of WZ-8A and the complemented

⁸http://fungi.ensembl.org/Fusarium_pseudograminearum/Info/Index

⁹<http://smart.embl-heidelberg.de>

¹⁰<https://toolkit.tuebingen.mpg.de/#/toolspsblast>

TABLE 1 | Primers used in the quantitative real-time PCR.

Name	Sequence (5'-3')	Description
FPSE_08050-RTF	AGGACAGAACATGGGGTCA	Quantitative real-time PCR primers for analysis of FPSE_08050 expression levels
FPSE_08050-RTR	GAGTACGAAACCAGATAGCATG	
FPSE_08176-RTF	CTATGAATTTGGAGGAACG	Quantitative real-time PCR primers for analysis of FPSE_08176 expression levels
FPSE_08176-RTR	TGCCAGTAGTCACGGATTTCC	
FPSE_02237-RTF	TTCTTGAGGACCGTATTGG	Quantitative real-time PCR primers for analysis of FPSE_02237 expression levels
FPSE_02237-RTR	TATGACGAACTGGAGGAGC	
FPSE_00389-RTF	AAGCCAGTTATTATTGTCGG	Quantitative real-time PCR primers for analysis of FPSE_00389 expression levels
FPSE_00389-RTR	TCTTTGATTCCCATTCTGC	
FPSE_05514-RTF	CTTGCCGTAGACGTCATC	Quantitative real-time PCR primers for analysis of FPSE_05514 expression levels
FPSE_05514-RTR	GTGTCCAGGAGTGGGTTGC	
FPSE_05576-RTF	AGGCGACGGTCTAGGAGTC	Quantitative real-time PCR primers for analysis of FPSE_05576 expression levels
FPSE_05576-RTR	TTGGGAATGAGAACAACAGC	
FPSE_08474-RTF	TCAGTGCCAGGAACCTAC	Quantitative real-time PCR primers for analysis of FPSE_08474 expression levels
FPSE_08474-RTR	TGGACTTCATCTGTACGC	
FPSE_05266-RTF	CCTTCAACCCGCCTCATA	Quantitative real-time PCR primers for analysis of FPSE_05266 expression levels
FPSE_05266-RTR	CTGGCTTCAACAATAGTGTCC	
FPSE_06206-RTF	GTCATGTCCTGCTCTTTACC	Quantitative real-time PCR primers for analysis of FPSE_06206 expression levels
FPSE_06206-RTR	GGTCAAGCCGAGGTACTC	
FPSE_07921-RTF	TGAGCTTCTACGAAACATC	Quantitative real-time PCR primers for analysis of FPSE_07921 expression levels
FPSE_07921-RTR	GCTTCACATTTGACCCAGT	
FPSE_04661-RTF	GCGTTGTTGATGCTTTGAG	Quantitative real-time PCR primers for analysis of FPSE_04661 expression levels
FPSE_04661-RTR	GACCTCCTGGACACCTGA	
MAT1-1-1-RTF	CGAACCTACTACTTGAAGC	Quantitative real-time PCR primers for analysis of MAT1-1-1 expression levels
MAT1-1-1-RTR	GTTACCAAAGTTGTCGTGA	
MAT1-1-2-RTF	CACGCTTGAGGTCTTACGC	Quantitative real-time PCR primers for analysis of MAT1-1-2 expression levels
MAT1-1-2-RTR	AGCAGATGGCAGATTTGGC	
MAT1-1-3-RTF	TCACTCGTGATCAATCTACT	Quantitative real-time PCR primers for analysis of MAT1-1-3 expression levels
MAT1-1-3-RTR	TTGTATCCAGGGTAAAGTC	

strain with almost no aerial hyphae that were common in the wild type strain (Figures 3A–C). $\Delta Fpppr1$ hyphae exhibited yellow color with several round sector branching points when grown to almost reach the edge of Petri dish for 10 d compared to the wild type WZ-8A and the complemented strain (Figure 3D). $\Delta Fpppr1$ spore morphology was abnormal with constriction in the septum and large portions of spores only had one septum and the germination rate was significantly reduced ($p < 0.05$) compared to WZ-8A and the complemented strain after 8 h in a drop of sterile water at 25°C (Figures 3E,G). Spore production in CMC media was reduced by 28-fold after a 4-d incubation compared with wild type (Figure 3F).

The $\Delta Fpppr1$ Functional Complementation and the *FpPpr1* Protein Localized to the Mitochondria

To functionally rescue the mutant, an *FpPpr1*-GFP fusion construct driven by a native promoter was generated and sequenced. When this GFP complementation construct was introduced to the protoplast of $\Delta Fpppr1-3$, the *FpPpr1*-GFP transformants grew on PDA plates containing G418 antibiotics for selection of transformants resistant to neomycin. The phenotypic defects of the

$\Delta Fpppr1-3$ mutant were successfully restored in verified complementation lines.

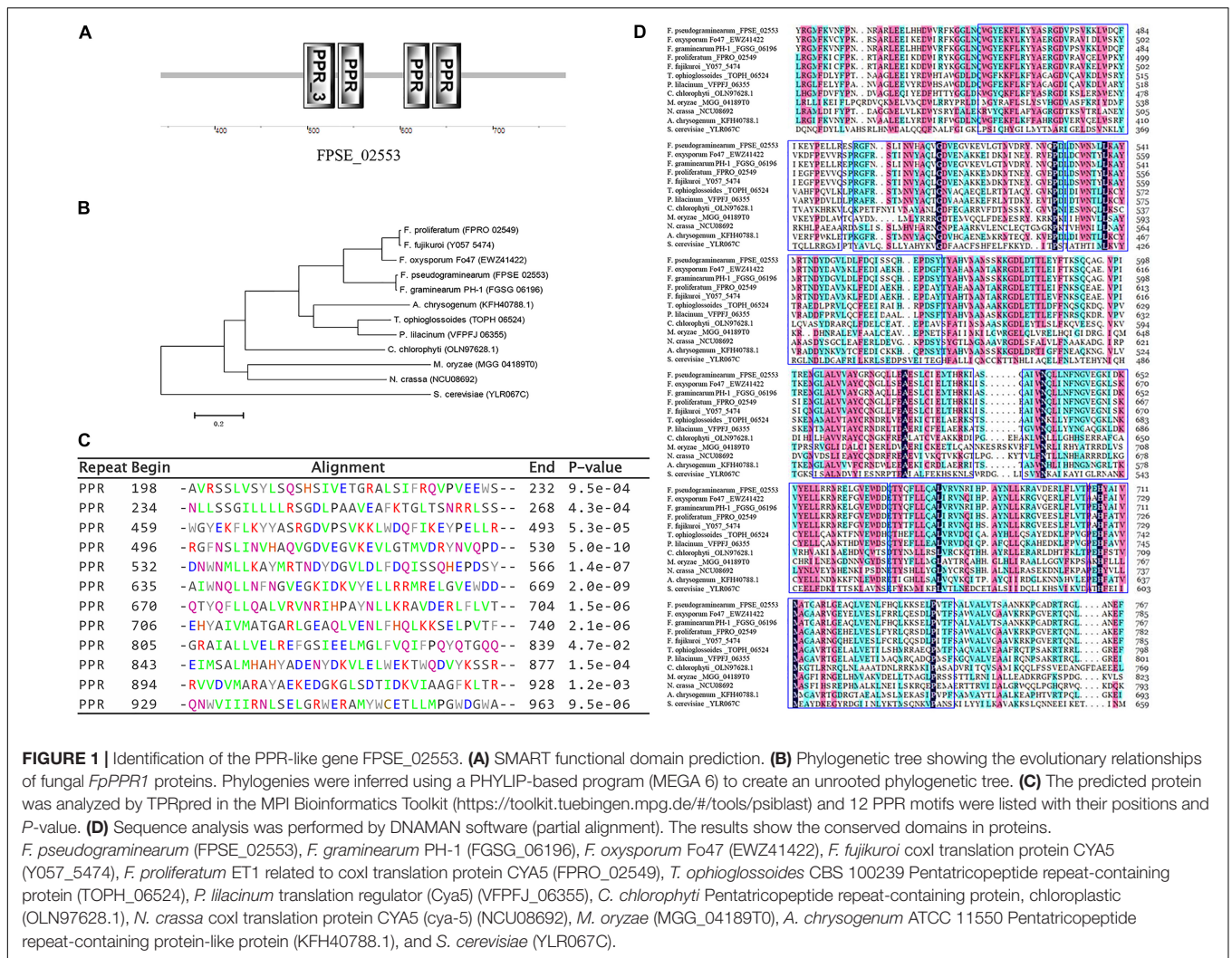
In order to determine the localization of the *FpPpr1* protein, the GFP complementation strain with a C-terminal GFP fusion to *FpPpr1* was examined under a Nikon microscope. GFP fluorescence was observed in an intracellular granule-like structure within spores and hyphae. As the *FpPPR1* proteins were predicted to be localized in the mitochondria by Wolf PSORT analysis¹¹ and a mitochondria localization signal was found in amino acids 1 to 30 of *FpPpr1*¹², further Mito-tracker Red CMXRos M7512 staining was performed. Some of the GFP signal overlapped with the Mito-tracker red signal, implying that *FpPPR1* was localized in the mitochondria, some signals appearing to localize in the cytosol (Figures 4A,B).

FpPPR1 Is Involved in Response to Cell Membrane and Cell Wall Stresses

On PDA containing 10 mM H₂O₂, $\Delta Fpppr1$ mutant growth had no obvious defect compared to WZ-8A and the complemented strain cFpppr1 (Figure 5A). In presence of 0.2 g/L Congo red and 0.05% SDS to stress the cell wall and cell membrane,

¹¹<https://www.genscript.com/wolf-psort.html?src=leftbar>

¹²<http://ipsort.hgc.jp/predict.cg>



respectively, colony growth was more stunted in $\Delta Fpppr1$ mutant compared to the other lines (Figure 5A). The calculated values showed a significantly increased inhibition rate ($p < 0.01$) in the $\Delta Fpppr1$ mutant under 0.2 g/L Congo red and 0.05% SDS, but the inhibition rate under 10 mM H₂O₂ was significantly lower ($p < 0.01$) than that of WZ-8A and the complemented strain cFpppr1 (Figure 5B).

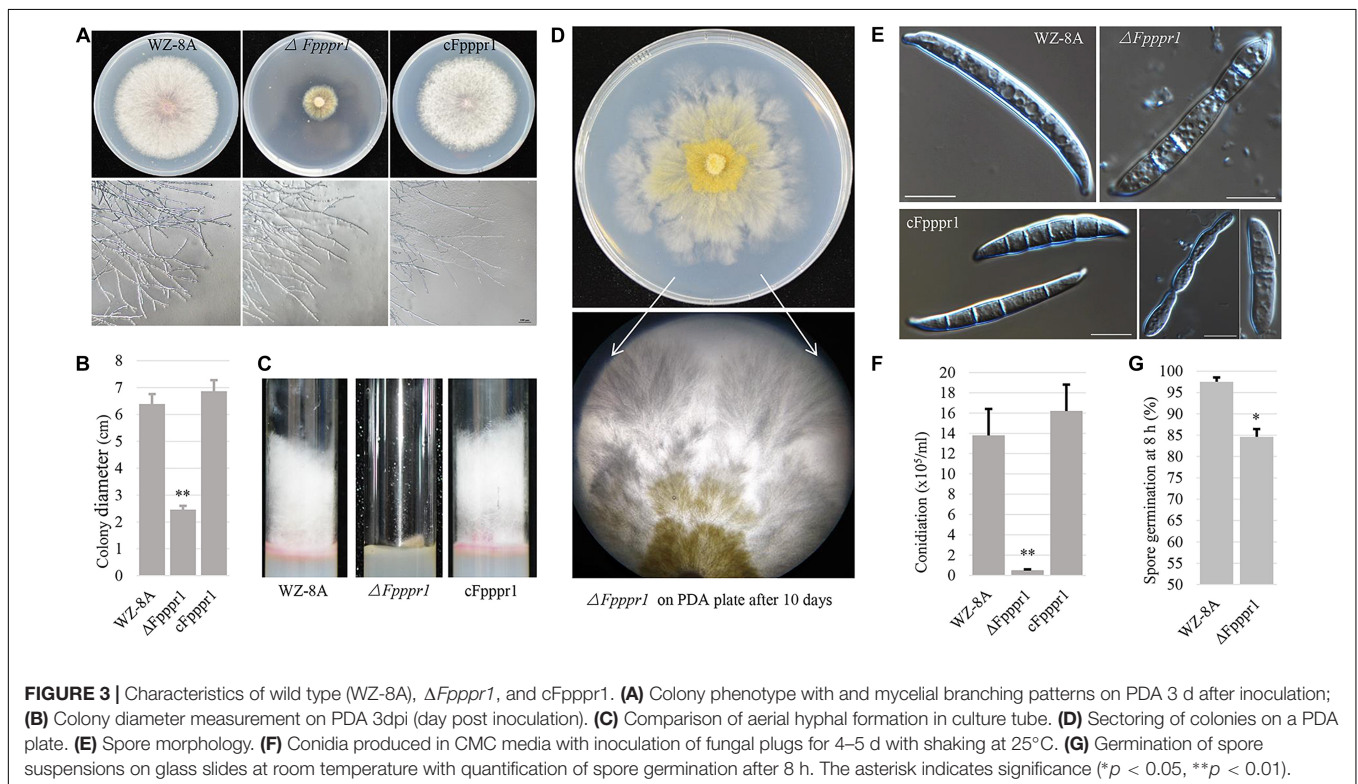
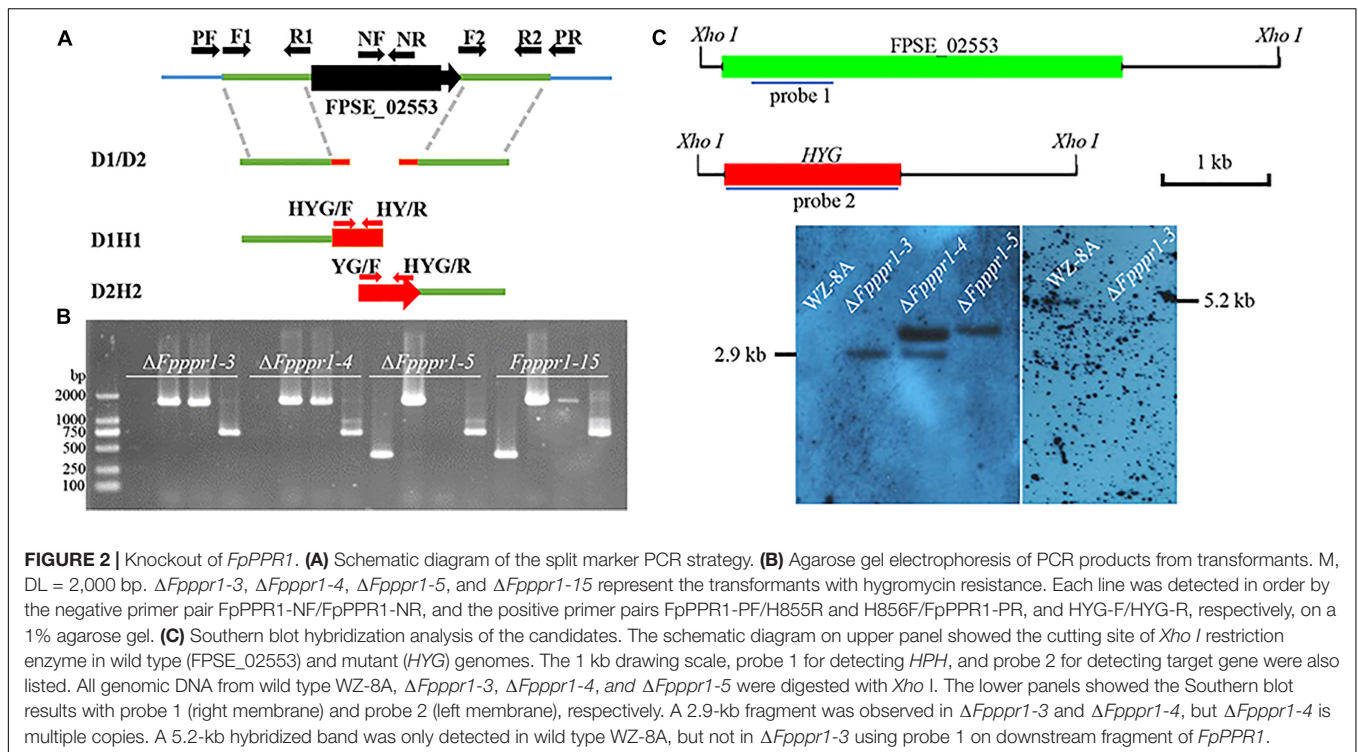
FpPPR1 Is Essential for Infecting Barley Leaves and Wheat Coleoptiles

To characterize the potential defects of host infection, fungal plugs of 3-day-old *F. pseudograminearum* were placed onto intact barley leaves attached to the bottom of the growth chamber facing up. WZ-8A and cFpppr1 caused large necrotic lesions in size on intact barley leaves by 3 d post-inoculation (dpi) after the fungal plugs were removed. In contrast, no lesions were found on the $\Delta Fpppr1$ mutant inoculated on intact barley leaves (Figure 6A). The fungal plugs were also put on intact wheat coleoptiles fixed horizontally on the bottom of a growth chamber. Brown or dark brown lesions were observed 3 d in

coleoptiles inoculated with WZ-8A and complemented strains, while no discoloration of coleoptiles was observed from the $\Delta Fpppr1$ mutant (Figure 6B). The transparent inner epidermis was stripped off and observed under a microscope. The infection mycelia from the mutant could be observed and showed no obvious morphological difference compared to wild type and cFpppr1 strains (Figure 6C). However, elongated mutant spore inoculation on coleoptiles did not cause lesions after 8 d (Figure 6D) or even 16 d (Figure 6E). Observing the inner epidermis of wheat coleoptile inoculated with 14 d, it was found that there were a lot of mycelium in it, but the wheat coleoptile did not show obviously dark brown or necroses symptom (Figure 6F and Supplementary Figure 3).

Genes Regulated by FpPPR1 Are Involved in Oxidoreductive Reactions, Mating, and Secondary Metabolism

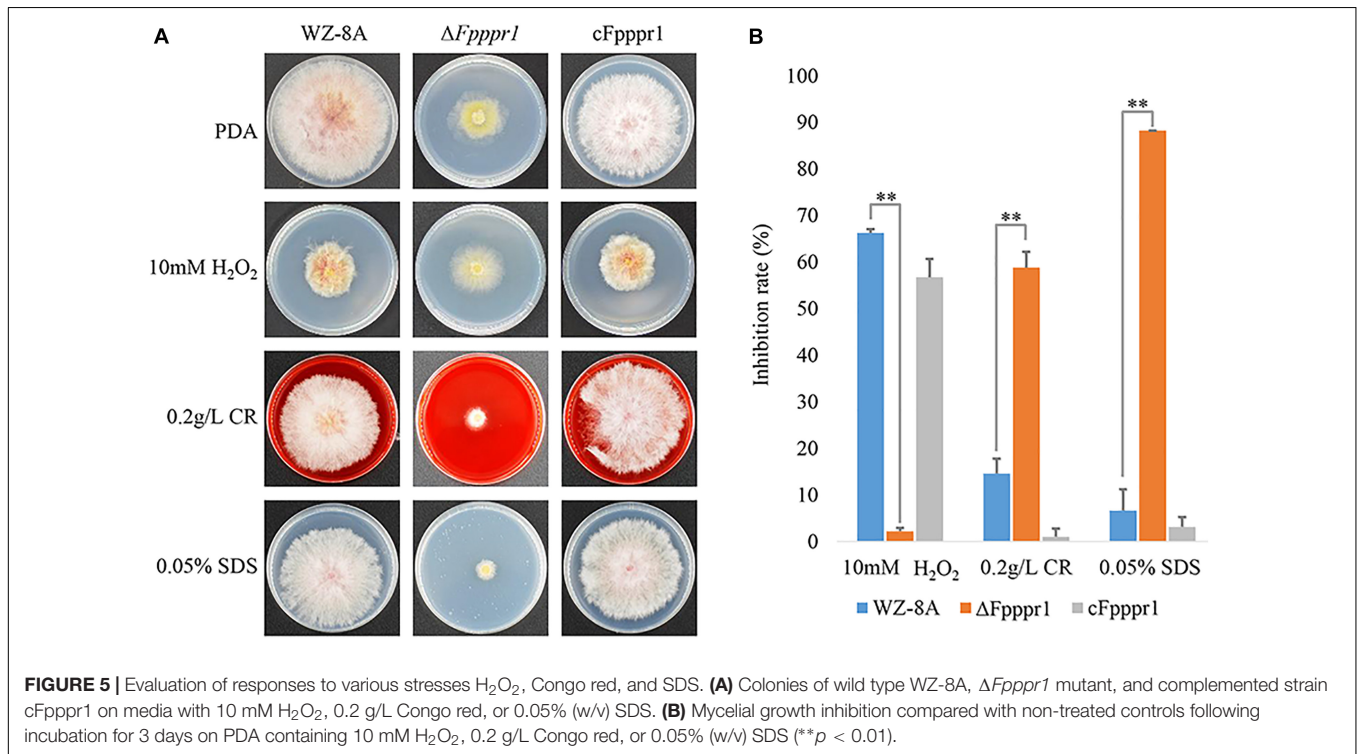
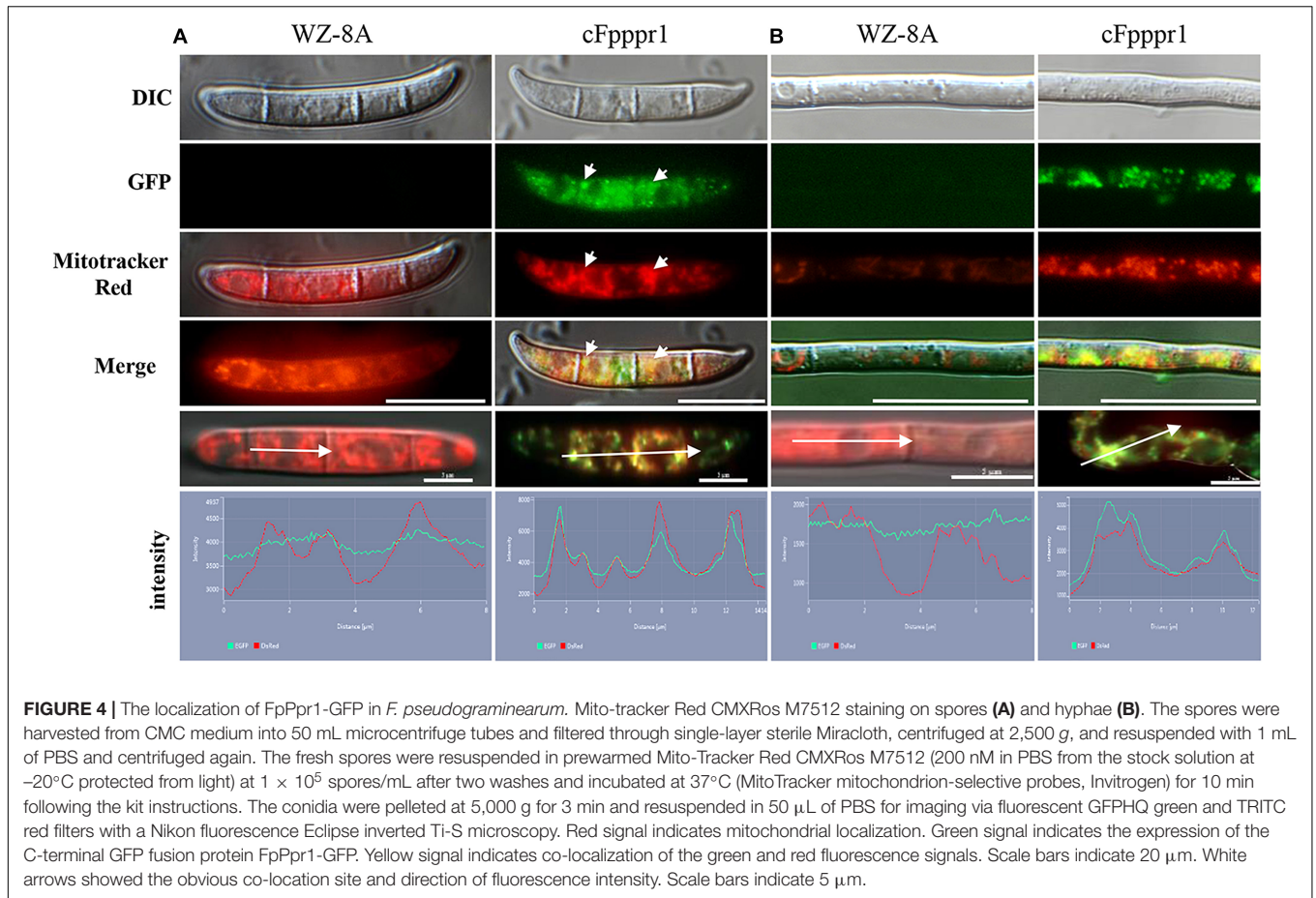
To explore the regulatory role of *FpPPR1* at a genome-wide scale, transcriptomic profiles were generated by the RNA-seq from wild type and the $\Delta Fpppr1$ mutant (RNA-seq data, submission No.



SUB7037132)¹³. A total of 1,367 genes were differentially down-regulated, while 1,333 genes were differentially up-regulated (all

the expression analysis at $p < 0.05$ and FDR < 0.05). Since FpPpr1-GFP largely localized to mitochondria, we noticed that down-regulated genes were enriched for molecular functions relevant to oxidoreductase activity during GO clustering

¹³<https://www.ncbi.nlm.nih.gov/Traces/study/?acc=PRJNA674906>



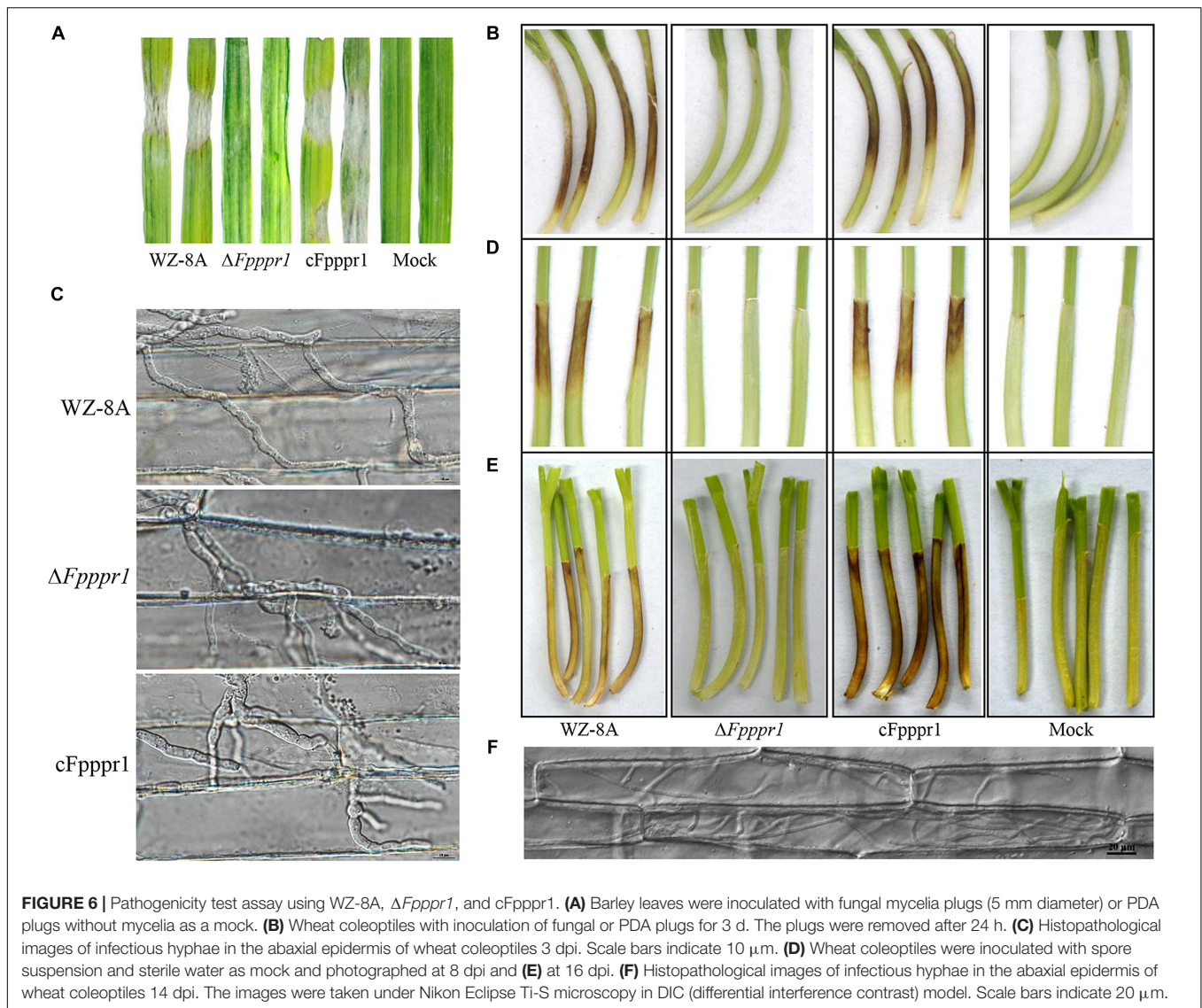


FIGURE 6 | Pathogenicity test assay using WZ-8A, $\Delta Fpppr1$, and cFpppr1. **(A)** Barley leaves were inoculated with fungal mycelia plugs (5 mm diameter) or PDA plugs without mycelia as a mock. **(B)** Wheat coleoptiles with inoculation of fungal or PDA plugs for 3 d. The plugs were removed after 24 h. **(C)** Histopathological images of infectious hyphae in the abaxial epidermis of wheat coleoptiles 3 dpi. Scale bars indicate 10 μm . **(D)** Wheat coleoptiles were inoculated with spore suspension and sterile water as mock and photographed at 8 dpi and **(E)** at 16 dpi. **(F)** Histopathological images of infectious hyphae in the abaxial epidermis of wheat coleoptiles 14 dpi. The images were taken under Nikon Eclipse Ti-S microscopy in DIC (differential interference contrast) model. Scale bars indicate 20 μm .

analysis (Figure 7A). Twenty-six cytochrome P450 genes were significantly down-regulated (9 in E-class group I, 7 in E-class group IV, and 10 in drug metabolism) (Figure 7B). We verified 10 genes encoding FAD or NAD-binding domain-containing oxidoreductases (Supplementary Table 2 with description) and FPSE_07921, encoding a putative E-class group I cytochrome P450, had significantly reduced expression levels after deletion of *FpPPR1* using qRT-PCR (Table 1 with primers; Figure 7C). Three genes, FPSE_11993, FPSE_12025, and FPSE_00773, encoding the 2Fe-2S iron-sulfur cluster binding domain proteins were also significantly down-regulated. Expression of FPSE_01622, encoding a thioredoxin TRX group I ortholog of TRX1 in *Magnaporthe oryzae*, was significantly reduced as well.

The three *MAT1-1* mating-type alleles, *FpMAT1-1-1*, *FpMAT1-1-2*, and *FpMAT1-1-3*, showed significantly down-regulated expression levels in mutant $\Delta Fpppr1$ (Figure 8A), which was also confirmed by qRT-PCR (Figure 8B). There were 21 gene-encoded putative heterokaryon incompatibility proteins

(HET) with significantly down-regulated expression levels in $\Delta Fpppr1$ (Figure 8C).

The *PKS12* (polyketide synthase 12) gene cluster, including *PKS12*, *aurF*, *aurJ*, *aurO*, *aurR1*, *aurR2*, *aurT*, and *gip1* in Figure 9A showed significantly down-regulated expression levels (Figure 9B), which was responsible for aurofusarin pigmentation the $\Delta Fpppr1$ mutant exhibited yellow coloration on PDA plates and in liquid CMC media (still sticky after several days incubation) (Figure 9C). Besides *PKS12*, *PKS2*, *PKS6*, *PKS10*, and *PKS14* also exhibited significantly lower expression levels in the $\Delta Fpppr1$ mutant.

DISCUSSION

In this study, we first characterized a putative *F. pseudograminearum* PPR gene *FpPPR1* in a filamentous phytopathogen, which encodes a protein containing 12 repeats

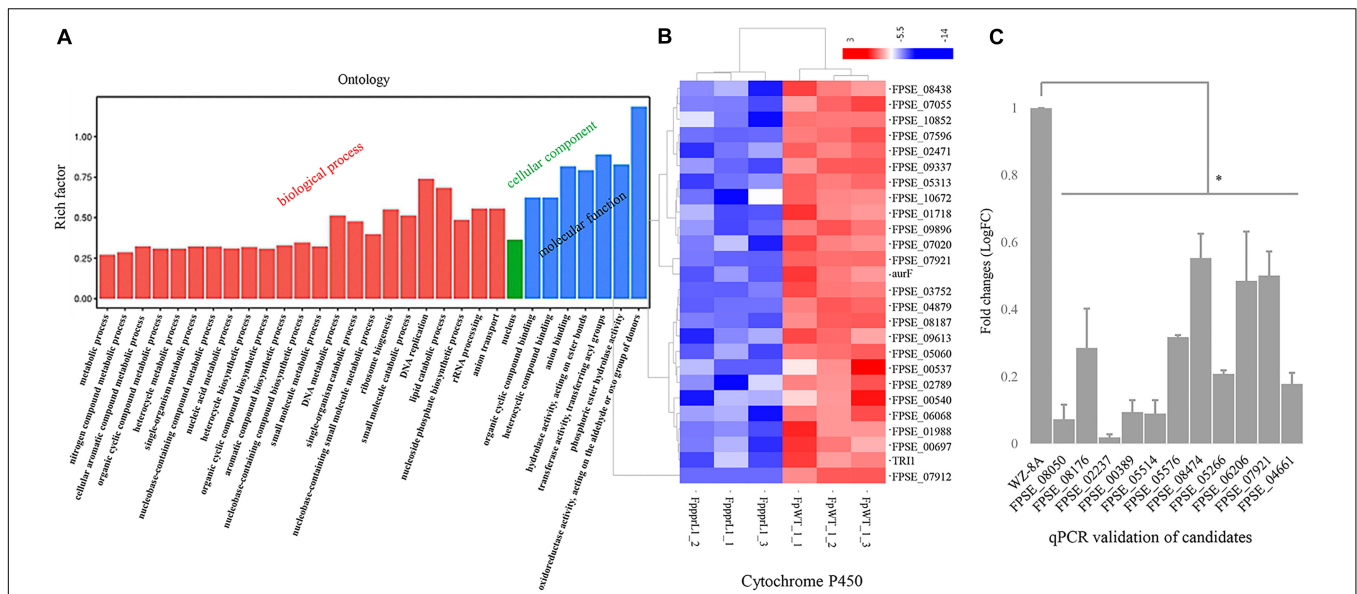


FIGURE 7 | Expression profiles of specific genes in the $\Delta Fppp1$ mutant compared to wild type. **(A)** Expression profiles of specific genes for $\Delta Fppp1$ and wild type strain WZ-8A in three biological replicates. The differentially expressed genes (DEGs) were in log₂ (fold change, FC) greater than 1.0 with a threshold at p-value and corrected p-value < 0.05 (False positive). **(B)** Heatmap for cytochrome P450 cluster. **(C)** Real time qRT-PCR for differentially down-regulated genes encoding oxidoreductases. First-strand cDNAs were synthesized using an RT-PCR kit as templates for qRT-PCR. The quantitative results are calculated and analyzed using the $2^{-\Delta\Delta Ct}$ method (*p < 0.05). FpppL1_1, FpppL1_2 and FpppL1_3 represent the sample names of the $\Delta Fppp1$ mutant strain for RNA-seq. FpWT_1_1, FpWT_1_2, and FpWT_1_3 represent the samples names of wild type strain WZ-8A for RNA-seq.

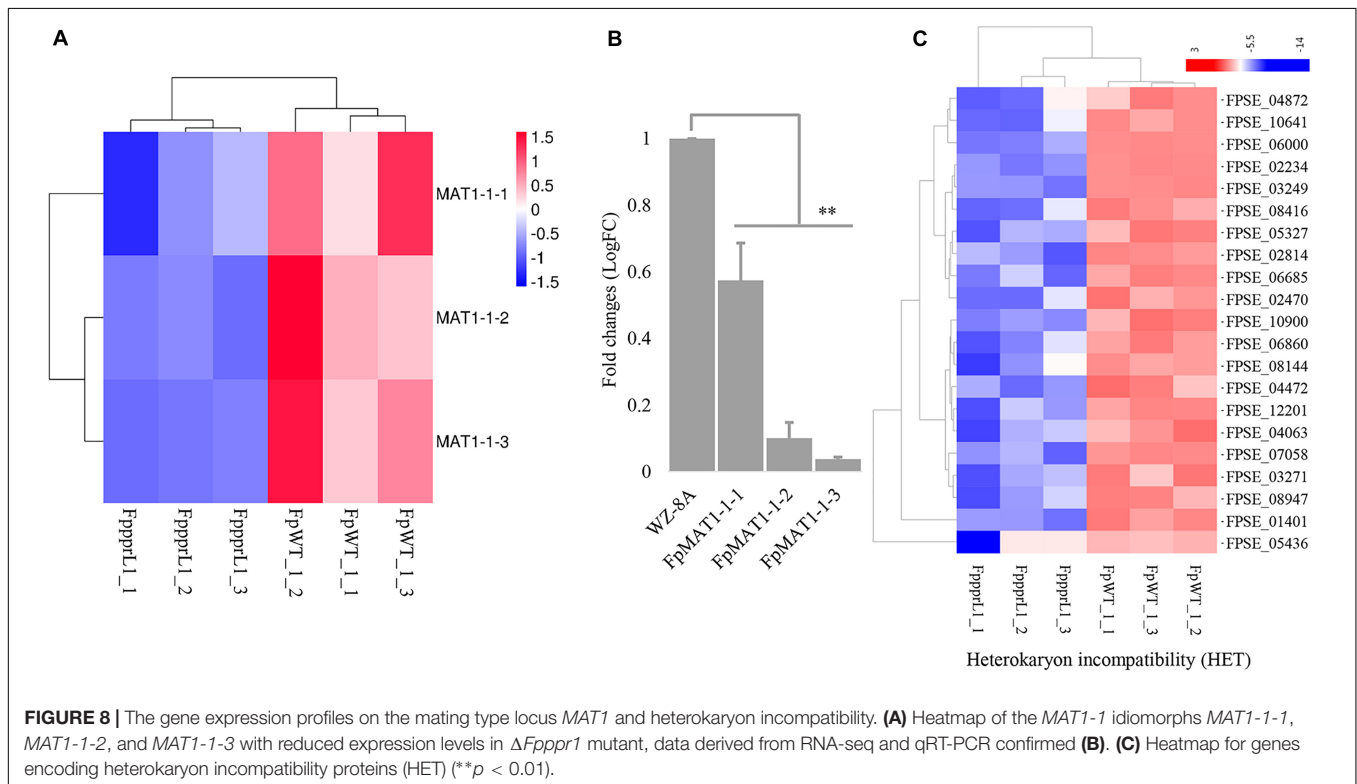
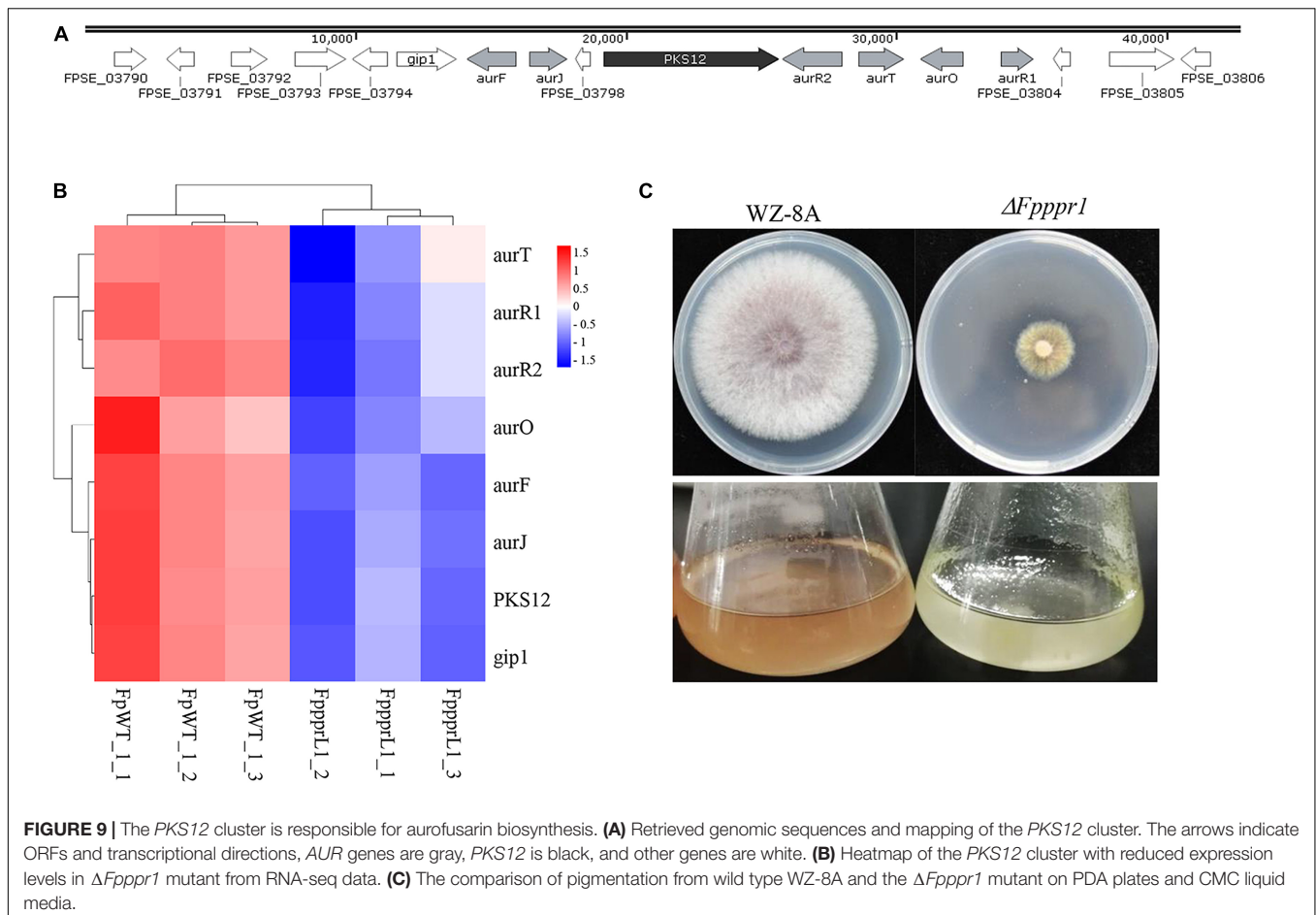


FIGURE 8 | The gene expression profiles on the mating type locus *MAT1* and heterokaryon incompatibility. **(A)** Heatmap of the *MAT1-1* idiomorphs *MAT1-1-1*, *MAT1-1-2*, and *MAT1-1-3* with reduced expression levels in $\Delta Fppp1$ mutant, data derived from RNA-seq and qRT-PCR confirmed **(B)**. **(C)** Heatmap for genes encoding heterokaryon incompatibility proteins (HET) (**p < 0.01).

of a degenerate 35-amino-acid motif. FpPpr1 is involved in multiple biological processes including aerial hyphae development, vegetative growth, asexual sporulation, mating

type gene expression, secondary metabolism and pathogenicity. Although more efforts are needed to validate these regulation pathways indicated by transcriptome data, we demonstrated



that the FpPpr1 are necessary for oxidoreductive system in mitochondria. We identified a disrupted gene with PPR motifs in *F. oxysporum* f. sp. *niveum* by ATMT (*Agrobacterium tumefaciens*-mediated transformation) displayed multiple defects including a reduced growth rate with white colony coloration, short and highly dense aerial hyphae, and reduced virulence on watermelon seedlings (**Supplemental Document**). The *FpPPR1* ortholog gene in *F. pseudograminearum* showed similar functions. Through DNAMAN alignment FpPpr1 shares 83.7% identity with putative *cya-5* orthologs in *Fusarium* spp. The *cya-5* pentatricopeptide repeat (PPR) protein in *Neurospora crassa* (Coffin et al., 1997), ortholog of yeast Pet309 PPR protein, which shared about 20% amino acid identity with FpPpr1, was required for post-transcriptional modification of COXI (cytochrome c oxidase subunit I), and the mutant was deficient in accumulation of mitochondria COXI pre-RNA and translation of COXI RNAs in yeast (Manthey et al., 2010). The spore germination of *N. crassa* was dependent upon the function of the cytochrome-mediated electron transport pathway within mitochondria. Transcriptomic analysis by RNA-seq from the $\Delta Fpppr1$ mutant and wild type revealed that large numbers of genes displayed differential expression after *FpPPR1* deletion. Among the genes with differentially down-regulated expression levels, clustering analysis mapped

the highest proportion of such genes into the gene products with oxidoreductive activity.

FpPpr1 contains a mitochondria localization signal and was found to be predominantly localized to said organelle. Previous studies have characterized the role of nuclear-encoded PPRs and similarly found mitochondria and plastid localization, with potential functions in targeting RNAs for RNA metabolism (Shikanai, 2006; Zehrmann et al., 2011; Giegä, 2013; Li and Jiang, 2018; Wang et al., 2018; Yan et al., 2018). However, FpPpr1 has not yet been shown to target RNAs, but assessing FpPpr1 binding of RNA in *F. pseudograminearum* is worth exploration. The PPR gene family in plants is involved in the response to environmental stimuli including biotic and abiotic stresses such as fungal infection, salicylic acid (SA), methyl jasmonate (MeJA), mechanical wounding, and cold and salinity stress (Kobayashi et al., 2007; Tang et al., 2010; Xing et al., 2018).

The $\Delta Fpppr1$ mutant exhibited reduced radial growth and colony sectoring. Li et al. (2008) reported that high oxidative stress, decreased membrane integrity, and DNA glycosylation in the mitochondria of mycelia contribute to the sectorization of colonies on PDA plate in the entomopathogenic soil fungus *Metarhizium anisopliae*. Mutation of the Mgv1 ortholog It2 from *Cryphonectria parasitica* led to abnormal cell wall integrity and sectorization (So et al., 2017). Overexpression of the

GIP2 transcription factor (also called aurR1) in aurofusarin biosynthesis caused sector formation and high pigmentation inhibited normal early vegetative growth in *Gibberella zeae* (Kim et al., 2006). The impaired aurofusarin biosynthesis likely led to the accumulation of the intermediate rubrofusarin, causing the yellow coloration on PDA plates. Our transcriptome data revealed similar defects in oxidative stress management and transmembrane components, and down-regulated aurofusarin biosynthesis in the mitochondria of mycelia, while the effects on membrane potential need to be measured to support links to previous findings.

The major pathogens of *Fusarium* crown rot, *F. pseudograminearum*, *F. graminearum*, and *F. culmorum*, all produce the red pigment aurofusarin, a dimeric polyketide naphthoquinone (Medentsev and Akimenko, 1998; Malz et al., 2005; Cambaza, 2018). A type I PKS (polyketide synthase) gene cluster, *PKS12*, is responsible for aurofusarin synthesis (Frandsen et al., 2006). There are 14 putative PKSs in *F. pseudograminearum* and 5 of them (*PKS2*, *PKS6*, *PKS10*, *PKS12*, and *PKS14*) were down-regulated in the $\Delta Fpppr1$ mutant. Malz et al. (2005) identified the *PKS12* gene cluster including 10 genes required for the biosynthesis of aurofusarin in *F. pseudograminearum* through *Agrobacterium tumefaciens*-mediated mutagenesis via T-DNA insertion. Our results suggest that FpPpr1 is at least involved in the regulation of the *PKS12* gene cluster in *F. pseudograminearum*. In *F. graminearum*, histone H3 lysine 4 methylation regulates the biosynthesis of aurofusarin (Liu et al., 2015; Cambaza, 2018). The *PKS12* gene seems not to affect pathogenicity in *F. pseudograminearum* (Malz et al., 2005), while more zearalenone (ZEA) was produced in the $\Delta pks12$ mutant. Aurofusarin negatively regulates zearalenone biosynthesis (Malz et al., 2005). *F. pseudograminearum* produces DON and ZEA as well (Blaney and Dodman, 2002), where DON plays an important role in virulence during *Fusarium* crown rot (Powell et al., 2017). Whether the attenuated virulence of the mutant has potential association with the mycotoxin reduction, DON and ZEA production in the $\Delta Fpppr1$ mutant needs to be measured.

F. pseudograminearum, also known as *Gibberella coronicola* (teleomorph), is a heterothallic fungus and the sexual process is controlled by opposite and distinct MAT idiomorphs, which include *MAT1-1* (*MAT1-1-1*, *MAT1-1-2*, and *MAT1-1-3* isoforms) and *MAT1-2* (*MAT1-2-1* and *MAT1-2-3* isoforms) loci in different strain, respectively (Gardiner et al., 2016). In the $\Delta Fpppr1$ mutant background, the expression levels of three mating type alleles in *MAT1-1* locus were significantly dropped off suggesting as a regulator in the sexual reproduction of *F. pseudograminearum*. Although there were still vary effects among the alleles. The smaller effect of FpPpr1 to *MAT1-1-1* was showed indicating that another factor exists through affecting this PPR gene. Whether the *MAT1-2* idiomorphs are regulated by *FpPPR1* still needs to be characterized. PPRs in plants have functions in restoring cytosolic male sterile (CMS) through regulating the genes related to CMS (Schmitz-Linneweber and Small, 2008; Lydiane et al., 2016). In *Ustilago maydis*, a dimorphic switch between yeast-like and filamentous growth is controlled by the mating-type loci (Wösten et al., 1996). Whether *FpPPR1* on regulation of

the mating type loci in *F. pseudograminearum* goes through aerial hyphae development still needs to be characterized. Sexual recognition is controlled by the mating-type locus and the vegetative recognition is controlled by heterokaryon incompatibility systems in filamentous ascomycetes (Saupe, 2000). In transcriptome data of $\Delta Fpppr1$ background, a group of genes encoding heterokaryon incompatibility proteins (HET) in mutant background were significantly reduced in expression level. The FpPpr1 upregulated the *HET* expression level might contribute the inhibition of heterokaryon formation in opposite MAT strains. In contrast, mutation of *FpPPR1* might result the heterokaryon formation, which might trigger parasexual process to be the potential genetic variation sources. The MAP kinase *MGV1* is essential for female fertility, heterokaryon formation, and plant infection in *F. graminearum* (Hou et al., 2002). The *mgv1* mutant was female sterile and its ortholog (FPSE_12362) was significantly down-regulated in the $\Delta Fpppr1$ mutant. The MAP kinase function is usually conserved in filamentous fungi. Therefore, FpPpr1 might potentially determine self/nonself recognition in vegetative, thereby contributing to genetic variation in *F. pseudograminearum*. Although the perithecia was not difficult to find in the field, it is still not such population like *F. graminearum*.

Aerial hyphae (or mycelia on substrate surface) are essential for asexual and sexual development to produce propagules and initiate opposite sexual recognition. The $\Delta Fpppr1$ mutant was defective in aerial hyphae formation. Sporulation was significantly reduced in the $\Delta Fpppr1$ mutant, which indicates the aerial hyphae were still available in CMC liquid media. Whether or not sexual crossing is lost needs to be confirmed. Hydrophobins are thought to reduce surface tension for hyphae growing into the air in filamentous bacteria and fungi (Wessels et al., 1991; Wösten and Willey, 2000; Bayry et al., 2012; Riquelme et al., 2018). In filamentous fungi, most autophagy genes, such as *TrATG5*, *ATG15*, *BcATG8*, *AoATG1*, *AoATG26*, *MoATG14*, and *MoATG24*, regulate aerial hyphae development and sporulation or conidia germination (Liu et al., 2011, 2017; He et al., 2013; Yanagisawa et al., 2013; Kikuma et al., 2017; Ren et al., 2018). Deletion of the related gene blocks significantly reduces aerial hyphae formation and sporulation (Kikuma et al., 2007; Lv et al., 2017; Ren et al., 2018; Liu et al., 2019). Most of the ATG genes are critical to selective mitochondrial autophagy for mitochondrial stasis (Marinkovic and Novak, 2015). The RNA-seq results from the $\Delta Fpppr1$ mutant did not reveal differentially expressed genes encoding hydrophobic proteins and ATG orthologs, which might indicate a novel mechanism through which *FpPPR1* regulates mating-type genes in *F. pseudograminearum* (Lugones et al., 2004; Elliot and Talbot, 2005). It is interesting that the key component, *MGV1*, in *F. graminearum* in the cell wall integrity (CWI) pathway Bck1-Mkk1-Slt2-Rlm1 was detected with a down-regulated expression level in $\Delta Fpppr1$ (Hou et al., 2002; Levin, 2005, 2011). The MAP kinase *mgv1* mutant produced fewer and shorter aerial hyphae with less pigmentation. Sensitivity to Congo red and SDS also suggested defects in the cell membrane and cell wall. The orthologs of AtSlt2 in *Alternaria alternata* (Yago et al., 2011), *Mpka* in *Aspergillus nidulans* (Bussink and Osmani, 1999),

Mgslt2 in *Mycosphaerella graminicola* (Mehrabi et al., 2006), Bmp3 in *Botrytis cinerea* (Rui and Hahn, 2007), FoSlt in *Fusarium oxysporum* f. sp. *cubense* (Ding et al., 2015), and CpSlt2 in *Cryphonectria parasitica* (So et al., 2017), and Mps1 in *M. oryzae* (Xu et al., 1998) shared similar phenotypes in mutants with fewer and shorter aerial hyphae of the colonies. Likewise, the deletion mutant of the ortholog *MgSlt2* in *Mycosphaerella graminicola* also did not produce aerial mycelia even after prolonged growth on PDA (Mehrabi et al., 2006). The *FpPPR1* gene in different filamentous phytopathogens might have a conserved function in regulating aerial hyphae development through the CMI MAPK pathway. The $\Delta Fpppr1$ mutant exhibited no pathogenicity when inoculated as a fungal mycelial plug and spore suspension onto plant tissue. Interestingly, if the fungal agar was not removed from coleoptiles, the $\Delta Fpppr1$ mutant could still cause lesions indicating the importance of aerial hyphae for infectious structure formation. *F. pseudograminearum* can form a foot-like appressorium and invade the neighboring cell for extension into host tissue. We speculate that the fewer, shortened aerial hyphae on the agar are capable of forming appressoria to penetrate the host epidermis. Along these lines, our histopathological images showed normal growth of infectious hyphae in the wheat coleoptile cells. This is similar to what was observed for *MgSlt2* mutants in *M. graminicola* which showed reduced virulence with no branching infectious hyphae (Mehrabi et al., 2006).

In summary, our findings uncovered new insight into pentatricopeptide repeat proteins in the filamentous phytopathogens *F. pseudograminearum* and *F. oxysporum* f. sp. *niveum*. We discovered multiple PPR functions related to growth, aerial hyphae development, sporulation, and regulation of mating type gene *MAT1-1*. To fully understand the roles of PPR proteins and to determine whether RNA processing also occurs in mitochondria in *F. pseudograminearum*, the seven remaining PPR proteins in *F. pseudograminearum* need to be characterized.

DATA AVAILABILITY STATEMENT

The original contributions presented in the study are publicly available. This data can be found here: <https://www.ncbi.nlm.nih.gov/Traces/study/?acc=PRJNA674906>.

AUTHOR CONTRIBUTIONS

LW, YZ, SX, and SL wrote the manuscript. HLL, HYL, and SD revised the manuscript. LW, YZ, and SX performed the majority of the experiments in *F. pseudograminearum* with participation from RK, MZ, MW, LC, and HY. SL performed all the experiments in *F. oxysporum* f. sp. *niveum*. All authors contributed to the article and approved the submitted version.

REFERENCES

Backhouse, D. (2014). Modelling the behaviour of crown rot in wheat caused by *Fusarium pseudograminearum*. *Aus. Plant Pathol.* 43, 15–23. doi: 10.1007/s13313-013-0247-6

FUNDING

This research was partially supported by the National Science Foundation (31871922), National Project of Grain Production of the Ministry of Science and Technology of China (2017YFD0301104), the National Special Fund for Agro-scientific Research in the Public Interest (201503112), and the National Science Foundation (31371902). Department of Education of Henan Province for the Basic Frontier and Key Laboratory Projects (grant no. 152300410073).

ACKNOWLEDGMENTS

We give thanks to Dr. Daniel Ebbolle (Texas A&M University, College Station, TX, United States) for critically reading the manuscript. UMI RNA-seq was performed by Seqhealth Technology Co., Ltd. (Wuhan, China) and we thank Kejun Xie from this company for his technical assistance.

SUPPLEMENTARY MATERIAL

The Supplementary Material for this article can be found online at: <https://www.frontiersin.org/articles/10.3389/fgene.2020.535622/full#supplementary-material>

Supplementary Figure 1 | Vectors used for *Agrobacterium tumefaciens*-mediated transformation of *Fusarium oxysporum* f. sp. *niveum* (FON) strain FON-11-06, the special structure of the T-DNA region in pATMT1-EGFP and pATMT1 vectors for high-efficiency nested inverse (HENI)-PCR, and a schematic diagram for identifying the sequences flanking the T-DNA region of interest. **(A)** pCambia1300 vector, **(B1)** pATMT1 vector, and **(B2)** pATMT1-EGFP vector; Panels **(B1)** and **(B2)** were suitable for HENI-PCR amplification of unknown sequences flanking both borders of T-DNA in transgenic FON mutants; **(C1–C3)** schematic diagram for identifying sequences flanking the T-DNA region of interest; **(D)** special T-DNA structure for HENI-PCR in pATMT1-EGFP vector and primer design. **(E)** Numbers 1 to 12 in panel **(C)** correspond to 12 primers, namely ILP, ILP1, IRP1, IRP2, ILP4, ILP3, ILP6, ILP5, IRP3, IRP4, ILP8, and ILP7, respectively.

Supplementary Figure 2 | Morphology and pathogenicity assay for the mutant W1005D in FON strain FON-11-06. **(A)** The wild type and mutant cultures on PDA plates after 7 d at room temperature. **(B)** The sprouting watermelon seeds were inoculated directly with 0.5 mL of the spore suspension at 1×10^5 /mL in the tray cells. The sterile water was dropped onto seeds as a mock control. The tray was kept in an incubator under 25/16°C day/night temperatures and a 12 h photoperiod for 12 d.

Supplementary Figure 3 | Histopathological images of infectious hyphae in the inner epidermis of wheat coleoptiles inoculated with $\Delta Fpppr1$ plugs 14 dpi. **(A)** Inoculation of wheat coleoptiles in a plastic tray and infectious hyphae expanding in host cells without discoloration **(B)**. Scale bars indicate 20 μ m.

Supplementary Table 1 | Primers used in this study for gene knockout.

Supplementary Table 2 | Expression profiles on oxidoreductive-related genes in $\Delta Fpppr1$ mutant.

Barkan, A., and Small, I. (2014). Pentatricopeptide repeat proteins in plants. *Ann. Rev. Plant Biol.* 65, 415–442. doi: 10.1146/annurev-arplant-050213-040159

Bayry, J., Aïmanianda, V., Guijarro, J. I., Sunde, M., and Latgé, J. P. (2012). Hydrophobins—Unique Fungal Proteins. *PLoS Pathog.* 8:e1002700. doi: 10.1371/journal.ppat.1002700

- Blaney, B. J., and Dodman, R. L. (2002). Production of zearalenone, deoxynivalenol, nivalenol, and acetylated derivatives by Australian isolates of *Fusarium graminearum* and *F. pseudograminearum* in relation to source and culturing conditions. *Aus. J. Agri. Res.* 53, 1317–1326. doi: 10.1071/ar02041
- Bovill, W. D., Horne, M., Herde, D., Davis, M., Wildermuth, G. B., Sutherland, M. W., et al. (2010). Pyramiding QTL increases seedling resistance to crown rot (*Fusarium pseudograminearum*) of wheat (*Triticum aestivum*). *Theor. Appl. Genet.* 121, 127–136. doi: 10.1007/s00122-010-1296-7
- Burgess, L. W., Klein, T. A., Bryden, W. L., and Tobin, N. F. (1987). Head blight of wheat caused by *Fusarium graminearum* group 1 in New South Wales in 1983. *Aus. Plant Pathol.* 16, 72–78. doi: 10.1071/APP98700
- Burgess, L. W., Backhouse, D., Swan, L. J., and Esdaile, R. J. (1996). Control of *Fusarium* crown rot of wheat by late stubble burning and rotation with sorghum. *Australas. Plant Pathol.* 25, 229–233. doi: 10.1071/AP96042
- Bussink, H. J., and Osmani, S. A. (1999). A mitogen-activated protein kinase (MPKA) is involved in polarized growth in the filamentous fungus, *Aspergillus nidulans*. *FEMS Microbiol. Lett.* 173, 117–125. doi: 10.1111/j.1574-6968.1999.tb13492.x
- Cambaza, E. (2018). Comprehensive description of *Fusarium graminearum* pigments and related compounds. *Foods* 7:165. doi: 10.3390/foods7100165
- Cao, S., Zhang, S., Hao, C., Liu, H., Xu, J. R., Jin, Q., et al. (2016). FgSsn3 kinase, a component of the mediator complex, is important for sexual reproduction and pathogenesis in *Fusarium graminearum*. *Sci. Rep.* 6:22333. doi: 10.1038/srep22333
- Catlett, N. L., Lee, B. N., Yoder, O. C., and Turgeon, B. G. (2003). Split-marker recombination for efficient targeted deletion of fungal genes. *Fungal Genet. Newslett.* 50, 9–11. doi: 10.4148/1941-4765.1150
- Chen, L., Geng, X., Ma, Y., Zhao, J., Li, T., Ding, S., et al. (2019c). Identification of basic helix-loop-helix transcription factors reveals candidate genes involved in pathogenicity of *Fusarium pseudograminearum*. *Can. J. Plant. Pathol.* 4, 200–208. doi: 10.1080/07060661.2018.1564941
- Chen, L. L., Geng, X. J., Ma, Y. M., Wang, L. M., Shi, Y., Li, H. L., et al. (2018). Identification and expression analysis of autophagy-related gene in *Fusarium pseudograminearum*. *Acta Phytotaxonom. Sinica* 48, 357–364.
- Chen, L., Geng, X., Ma, Y., Zhao, J., Chen, W., Xing, X., et al. (2019a). The ER luminal Hsp70 protein FpLhs1 is important for conidiation and plant infection in *Fusarium pseudograminearum*. *Front. Microbiol.* 10:1401. doi: 10.3389/fmicb.2019.01401
- Chen, L., Ma, Y., Zhao, J., Geng, X., Chen, W., Ding, S., et al. (2019b). The bZIP transcription factor FpAda1 is essential for fungal growth and conidiation in *Fusarium pseudograminearum*. *Curr. Genet.* 66, 507–515. doi: 10.1007/s00294-019-01042-1
- Chen, L., Tong, Q., Zhang, C., and Ding, K. (2019). The transcription factor FgCrz1A is essential for fungal development, virulence, deoxynivalenol biosynthesis and stress responses in *Fusarium graminearum*. *Curr. Genet.* 65:153. doi: 10.1007/s00294-018-0853-5
- Coffin, J. W., Dhillon, R., Ritzel, R. G., and Nargang, F. E. (1997). The *Neurospora crassa* cya-5 nuclear gene encodes a protein with a region of homology to the *Saccharomyces cerevisiae* PET309 protein and is required in a post-transcriptional step for the expression of the mitochondrially encoded COXI protein. *Curr. Genet.* 32, 273–280. doi: 10.1007/s002940050277
- Deng, Y. Y., Li, W., Zhang, P., Sun, H. Y., Zhang, X. X., Zhang, A. X., et al. (2020). *Fusarium pseudograminearum* as an emerging pathogen of crown rot of wheat in eastern China. *Plant Pathol.* 62:13122. doi: 10.1111/ppa.13122
- Ding, Z., Li, M., Sun, F., Xi, P., Sun, L., Zhang, L., et al. (2015). Mitogen-activated protein kinases are associated with the regulation of physiological traits and virulence in *Fusarium oxysporum* f. sp. *cubense*. *PLoS One* 10:e0122634. doi: 10.1371/journal.pone.0122634
- Dodman, R. L., and Wildermuth, G. B. (1989). The effect of stubble retention and tillage practices in wheat and barley on crown rot caused by *Fusarium graminearum* group 1. *Plant Prot. Q.* 4, 98–99.
- Elliot, M. A., and Talbot, N. J. (2005). Building filaments in the air: aerial morphogenesis in bacteria and fungi. *Curr. Opin. Microbiol.* 7, 594–601. doi: 10.1016/j.mib.2004.10.013
- Frandsen, R. J. N., Nielsen, N. J., Maolanon, N., Srensen, J. C., and Giese, H. (2006). The biosynthetic pathway for aurofusarin in *Fusarium graminearum* reveals a close link between the naphthoquinones and naphthopyrones. *Mol. Microbiol.* 61, 1069–1080. doi: 10.1111/j.1365-2958.2006.05295.x
- Gardiner, D. M., Benfield, A. H., Stiller, J., Stephen, S., Aitken, K., Liu, C., et al. (2016). A high resolution genetic map of the cereal crown rot pathogen *Fusarium pseudograminearum* provides a near complete genome assembly. *Mol. Plant Pathol.* 19, 217–226. doi: 10.1111/mpp.12519
- Gardiner, D. M., McDonald, M. C., Covarelli, L., Solomon, P. S., Rusu, A. G., Marshall, M., et al. (2012). Comparative pathogenomics reveals horizontally acquired novel virulence genes in fungi infecting cereal hosts. *Plos Pathog.* 8:e1002952. doi: 10.1371/journal.ppat.1002952
- Giegä, P. (2013). Pentatricopeptide repeat proteins: a set of modular RNA-specific binders massively used for organelle gene expression. *RNA Biol.* 10, 1417–1418. doi: 10.4161/rna.26081
- He, Y., Deng, Y. Z., and Naqvi, N. I. (2013). Atg24-assisted mitophagy in the foot cells is necessary for proper asexual differentiation in *Magnaporthe oryzae*. *Autophagy* 9, 1818–1827. doi: 10.4161/auto.26057
- Herbert, C. J., Golik, P., and Bonnefoy, N. (2013). Yeast PPR proteins, watchdogs of mitochondrial gene expression. *RNA Biol.* 10, 1477–1494. doi: 10.4161/rna.25392
- Hou, Z., Xue, C., Peng, Y., Katan, T., Kistler, H. C., Xu, J. R., et al. (2002). A mitogen-activated protein kinase gene (MGV1) in *Fusarium graminearum* is required for female fertility, heterokaryon formation and plant infection. *Mol. Plant Microb. Interact.* 15:1119. doi: 10.1094/MPMI.2002.15.11.1119
- Ji, L. J., Kong, L. X., Li, Q. S., Wang, L. S., Chen, D., Ma, P., et al. (2015). First report of *Fusarium pseudograminearum* causing *Fusarium* head blight of wheat in Hebei province, China. *Plant Dis.* 100:220. doi: 10.1094/PDIS-06-15-0643-PDN
- Kang, R., Li, G., Zhang, M., Zhang, P., Wang, L., Zhang, Y., et al. (2020). Expression of *Fusarium pseudograminearum* FpNPS9 in wheat plant and its function in pathogenicity. *Curr. Genet.* 66, 229–243. doi: 10.1007/s00294-019-01017-2
- Kazan, K., and Gardiner, D. (2017). *Fusarium* crown rot caused by *Fusarium pseudograminearum* in cereal crops: recent progress and future prospects. *Mol. Plant Pathol.* 19, 1547–1562. doi: 10.1111/mpp.12639
- Kettle, A. J., Batley, J., Benfield, A. H., Manners, J. M., Kazan, K., Gardiner, D. M., et al. (2015a). Degradation of the benzoxazolinone class of phytoalexins is important for virulence of *Fusarium pseudograminearum* towards wheat. *Mol. Plant Pathol.* 16, 946–962. doi: 10.1111/mpp.12250
- Kettle, A. J., Carere, J., Batley, J., Benfield, A. H., Manners, J. M., Kazan, K., et al. (2015b). A gamma-lactamase from cereal infecting *Fusarium* spp. catalyses the first step in the degradation of the benzoxazolinone class of phytoalexins. *Fungal Genet. Biol.* 83, 1–9. doi: 10.1016/j.fgb.2015.08.005
- Kettle, A. J., Carere, J., Batley, J., Manners, J. M., Kazan, K., Gardiner, D. M., et al. (2016). The Fdb3 transcription factor of the *Fusarium* Detoxification of Benzoxazolinone gene cluster is required for MBOA but not BOA degradation in *Fusarium pseudograminearum*. *Fungal Genet. Biol.* 88, 44–53. doi: 10.1016/j.fgb.2016.01.015
- Kikuma, T., Arioka, M., and Kitamoto, K. (2007). Autophagy during sporulation and spore germination in filamentous fungi. *Autophagy* 3, 128–129. doi: 10.4161/auto.3560
- Kikuma, T., Tadokoro, T., Maruyama, J. I., and Kitamoto, K. (2017). AoAtg26, a putative sterol glucosyltransferase, is required for autophagic degradation of peroxisomes, mitochondria, and nuclei in the filamentous fungus *Aspergillus oryzae*. *Biosci. Biotechnol. Biochem.* 81, 384–395. doi: 10.1080/09168451.2016.1240603
- Kim, J. E., Jin, J., Kim, H., Kim, J. C., Yun, S. H., Lee, Y. W., et al. (2006). GIP2, a putative transcription factor that regulates the aurofusarin biosynthetic gene cluster in *Gibberella zeae*. *Appl. Environ. Microbiol.* 72, 1645–1652. doi: 10.1128/AEM.72.2.1645-1652.2006
- Kobayashi, K., Suzuki, M., Tang, J., Nagata, N., Ohyama, K., Seki, H., et al. (2007). Lovastatin insensitive 1, a novel pentatricopeptide repeat protein, is a potential regulatory factor of isoprenoid biosynthesis in Arabidopsis. *Plant Cell. Physiol.* 48, 322–331. doi: 10.1093/pcp/pcm005
- Lee, S. B., Milgroom, M. G., and Taylor, J. W. (1988). A rapid, high yield mini-prep method for isolation of total genomic DNA from fungi. *Fungal Genet. Rep.* 35, 23–24. doi: 10.4148/1941-4765.1531
- Levin, D. E. (2005). Cell wall integrity signaling in *Saccharomyces cerevisiae*. *Microbiol. Mol. Biol. Rev.* 69, 262–291. doi: 10.1128/MMBR.69.2.262-291.2005
- Levin, D. E. (2011). Regulation of cell wall biogenesis in *Saccharomyces cerevisiae*: the cell wall integrity signaling pathway. *Genetics* 189, 1145–1175. doi: 10.1534/genetics.111.128264

- Li, H., He, X., Ding, S., Yuan, H., and Chen, L. (2016). First report of *Fusarium culmorum* causing crown rot of wheat in China. *Plant Dis.* 100:2532. doi: 10.1094/PDIS-05-16-0723-PDN
- Li, L., Pischetsrieder, M., St. Leger, R. J., and Wang, C. (2008). Associated links among mtDNA glycation, oxidative stress and colony sectorization in *Metarhizium anisopliae*. *Fungal Genet. Biol.* 45, 1300–1306. doi: 10.1016/j.fgb.2008.06.003
- Li, X. L., and Jiang, Y. S. (2018). The roles of PPR proteins on plant organelle RNA processing. *Chin. J. Biochem. Mol. Biol.* 34, 713–738. doi: 10.13865/j.cnki.cjmb.2018.07.04
- Li, Y., Zhou, H., Li, H. (2017). Detection of wheat ear mold in henan. *Henan Sci.* 35, 742–749. doi: 10.3969/j.issn.1004-3918.2017.05.013
- Lightowlers, R. N., and Chrzanowska-Lightowlers, Z. M. (2008). PPR (pentatricopeptide repeat) proteins in mammals: important aids to mitochondrial gene expression. *Biochem. J.* 416:e5. doi: 10.1042/BJ20081942
- Liu, C., Ogonnaya, F. C., and Bürstmayr, H. (2015). Resistance to *Fusarium* crown rot in wheat and barley: a review. *Plant Breeding* 134, 365–372. doi: 10.1111/pbr.12274
- Liu, N., Ren, W., Li, F., Chen, C., and Ma, Z. (2019). Involvement of the cysteine protease *bcatg4* in development and virulence of *Botrytis cinerea*. *Curr. Genet.* 65, 293–300. doi: 10.1007/s00294-018-0882-0
- Liu, X. H., Yang, J., He, R. L., Lu, J. P., Zhang, C. L., Lu, S. L., et al. (2011). An autophagy gene, *TrATG5*, affects conidiospore differentiation in *Trichoderma reesei*. *Res. Microbiol.* 162, 756–763. doi: 10.1016/j.resmic.2011.06.011
- Liu, X. H., Zhao, Y. H., Zhu, X. M., Zeng, X. Q., Huang, L. Y., Dong, B., et al. (2017). Autophagy-related protein *MoAtg14* is involved in differentiation, development and pathogenicity in the rice blast fungus *Magnaporthe oryzae*. *Sci. Rep.* 7:40018. doi: 10.1038/srep40018
- Livak, K. J. and Schmittgen, T. D. (2001). Analysis of relative gene expression data using real-time quantitative PCR and the $2^{-\Delta\Delta Ct}$ method. *Methods* 25, 402–408. doi: 10.1006/meth.2001.1262
- Lugones, L. G., Jong, J. F. D., Vries, O. M. H. D., Jalving, R., and Wsten, H. A. B. (2004). The SC15 protein of *Schizophyllum commune* mediates formation of aerial hyphae and attachment in the absence of the SC3 hydrophobin. *Mol. Microbiol.* 53, 707–716. doi: 10.1111/j.1365-2958.2004.04187.x
- Lurin, C., Andrés, C., Aubourg, S., Bellaoui, M., Bitton, F., Bruyère, C., et al. (2004). Genome-wide analysis of Arabidopsis pentatricopeptide repeat proteins reveals their essential role in organelle biogenesis. *Plant Cell* 16, 2089–2103. doi: 10.1105/tpc.104.022236
- Lv, W. Y., Wang, C. Y., Yang, N., Que, Y. W., Talbot, N. J., Wang, Z. Y., et al. (2017). Genome-wide functional analysis reveals that autophagy is necessary for growth, sporulation, deoxynivalenol production and virulence in *Fusarium graminearum*. *Sci. Rep.* 7:11062. doi: 10.1038/s41598-017-11640-z
- Lydiane, G., Brown, G. G., and Hakim, M. (2016). The propensity of pentatricopeptide repeat genes to evolve into restorers of cytoplasmic male sterility. *Front. Plant Sci.* 7:1816. doi: 10.3389/fpls.2016.01816
- Malz, S., Grell, M. N., Thrane, C., Maier, F. J., Rosager, P., Felk, A., et al. (2005). Identification of a gene cluster responsible for the biosynthesis of aurofusarin in the *Fusarium graminearum* species complex. *Fungal Genet. Biol.* 42, 420–433. doi: 10.1016/j.fgb.2005.01.010
- Manthey, G. M., Przybyla-Zawislak, B. D., and Mcewen, J. E. (2010). The *Saccharomyces cerevisiae* Pet309 protein is embedded in the mitochondrial inner membrane. *FEBS J.* 255, 156–161. doi: 10.1046/j.1432-1327.1998.2550156.x
- Marinkovic, M. and Novak, M. I. (2015). The role of autophagy receptors in mitophagy. *Autophagy Cancer Other Pathol. Inflammation Immun. Infect. Aging* 6, 243–256. doi: 10.1016/B978-0-12-801032-7.00017-4
- McCarthy, D. J., Chen, Y., and Smyth, G. K. (2012). “Differential expression analysis of multifactor RNA-Seq experiments with respect to biological variation.” *Nucleic Acids Res.* 40, 4288–4297. doi: 10.1093/nar/gks042
- Medentsev, A. G., and Akimenko, V. K. (1998). Naphthoquinone metabolites of the fungi. *Phytochemistry*, 47, 935–959. doi: 10.1016/s0031-9422(98)80053-8
- Mehrabi, R., Theo, V. D. L., Waalwijk, C., and Kema, G. H. J. (2006). *MgSlit2*, a cellular integrity map kinase gene of the fungal wheat pathogen *Mycosphaerella graminicola*, is dispensable for penetration but essential for invasive growth. *Mol. Plant Microb. Inter.* 19, 389–398. doi: 10.1094/MPMI-19-0389
- Miedaner, T., Cumagun, C. J. R., and Chakraborty, S. (2010). Population genetics of three important head blight pathogens *Fusarium graminearum*, *F. pseudograminearum* and *F. culmorum*. *J. Phytopathol.* 156, 129–139. doi: 10.1111/j.1439-0434.2007.01394.x
- Moseler, R., V. Solotoff, and U. Schulte. (2012). Two pentatricopeptide repeat proteins are essential for biogenesis of the NADH:ubiquinone oxidoreductase from the filamentous fungus *Neurospora crassa*. *BBA - Bioenerget.* 1817, S69–S70. doi: 10.1016/j.bbabo.2012.06.196
- Murray, G. M., and Brennan, J. P. (2009). The current and potential costs from diseases of wheat in Australia. (Grains Research and Development Corporation: Barton, ATC, Australia).
- Obanor, F., Neate, S., Simpfendorfer, S., Sabburg, R., Wilson, P., Chakraborty, S., et al. (2013). *Fusarium graminearum* and *Fusarium pseudograminearum* caused the 2010 head blight epidemics in Australia. *Plant Pathol.* 62, 79–91. doi: 10.1111/j.1365-3059.2012.02615.x
- Powell, J. J., Carere, J., Fitzgerald, T. L., Stiller, J., Covarelli, L., Xu, Q., et al. (2017). The *Fusarium* crown rot pathogen *Fusarium pseudograminearum* triggers a suite of transcriptional and metabolic changes in bread wheat (*Triticum aestivum* L.). *Ann. Bot.* 119, 853–867. doi: 10.1093/aob/mcw207
- Ren, W., Liu, N., Sang, C., Shi, D., and Chen, W. (2018). The autophagy gene *BcATG8* regulates vegetative differentiation and plant infection of *Botrytis cinerea*. *Appl. Environ. Microbiol.* 84:e02455-17. doi: 10.1128/AEM.02455-17
- Riquelme, M., Aguirre, J., Bartnicki-Garcia, S., Braus, G. H., Feldbrugge, M., Fleig, U., et al. (2018). Fungal morphogenesis, from the polarized growth of hyphae to complex reproduction and infection structures. *Microbiol. Mol. Biol. Rev.* 82:e00068-17. doi: 10.1128/MMBR.00068-17
- Robinson, M. D., McCarthy, D. J., and Smyth, G. K. (2010). edgeR: a Bioconductor package for differential expression analysis of digital gene expression data. *Bioinformatics* 26, 139–140. doi: 10.1093/bioinformatics/btp616
- Rui, O., and Hahn, M. (2007). The SlT2-type MAP kinase *Bmp3* of *Botrytis cinerea* is required for normal saprotrophic growth, conidiation, plant surface sensing and host tissue colonization. *Mol. Plant Pathol.* 8, 173–184. doi: 10.1111/j.1364-3703.2007.00383.x
- Saube, S. J. (2000). Molecular genetics of heterokaryon incompatibility in filamentous ascomycetes. *Microbiol. Mol. Biol. Rev.* 64, 489–502. doi: 10.1128/mmr.64.3.489-502.2000
- Schmitz-Linneweber, C., and Small, I. (2008). Pentatricopeptide repeat proteins: a socket set for organelle gene expression. *Trends Plant Sci.* 13, 663–670. doi: 10.1016/j.tplants.2008.10.001
- Shikanai, T. (2006). RNA editing in plant organelles: machinery, physiological function and evolution. *Cell. Mol. Life Sci.* 63, 698–708. doi: 10.1007/s00018-005-5449-9
- Small, I. D., and Peeters, N. (2000). The PPR motif - a TPR-related motif prevalent in plant organellar proteins. *Trends Biochem. Sci.* 25, 45–47. doi: 10.1016/S0968-0004(99)01520-0
- Smiley, R. W., Gourlie, J. A., Easley, S. A., Patterson, L. M., and Whittaker, R. G. (2005). Crop damage estimates for crown rot of wheat and barley in the Pacific Northwest. *Plant Dis.* 89, 595–604. doi: 10.1094/PD-89-0595
- So, K. K., Ko, Y. H., Chun, J., Kim, J. M., and Kim, D. H. (2017). Mutation of the SlT2 ortholog from *Cryphonectria parasitica* results in abnormal cell wall integrity and sectorization with impaired pathogenicity. *Sci. Rep.* 7:9038. doi: 10.1038/s41598-017-09383-y
- Su, Y., Chen, J., and Huang, Y. (2018). Disruption of *ppr3*, *ppr4*, *ppr6*, or *ppr10* induces flocculation and filamentous growth in *Schizosaccharomyces pombe*. *FEBS Microbiol. Lett.* 365:fny141. doi: 10.1093/femsle/fny141
- Su, Y., Yang, Y., and Huang, Y. (2017). Loss of *ppr3*, *ppr4*, *ppr6*, or *ppr10* perturbs iron homeostasis and leads to apoptotic cell death in *Schizosaccharomyces pombe*. *FEBS J.* 284:324. doi: 10.1111/febs.13978
- Summerell, B. A., and Burgess, L. W. (1988). Stubble management practices and the survival of *Fusarium graminearum* group 1 in wheat stubble residues. *Aus. Plant Pathol.* 17, 88–93. doi: 10.1071/AP9880088
- Tang, J. W., Kobayashi, K., Suzuki, M., Matsumoto, S. and Muranaka, T. (2010). The mitochondrial PPR protein LOVASTATIN INSENSITIVE 1 plays regulatory roles in cytosolic and plastidial isoprenoid biosynthesis through RNA editing. *Plant J.* 61, 456–466. doi: 10.1111/j.1365-313X.2009.04082.x
- Villagrasa, M., Guillamon, M., Labandeira, A., Taberner, A., Eljarrat, E., Barcelo, D., et al. (2006). Benzoxazinoid allelochemicals in wheat: distribution among foliage, roots, and seeds. *J. Agri. Food Chem.* 54, 1009–1015. doi: 10.1021/jf050898h

- Wang, L. M., Zhang, Y. F., Du, Z. L., Kang, R. J., Chen, L. L., Xing, X. P., et al. (2017). FpPDE1 function of *Fusarium pseudograminearum* on pathogenesis in wheat. *J. Integr. Agri.* 16, 2504–2512. doi: 10.1016/S2095-3119(17)61689-7
- Wang, Y., Yan, J., Zhang, Q., Ma, X., Zhang, J., Su, M., et al. (2017). The *Schizosaccharomyces pombe* PPR protein Ppr10 associates with a novel protein Mpa1 and acts as a mitochondrial translational activator. *Nucleic Acids Res.* 45, 3323–3340. doi: 10.1093/nar/gkx127
- Wang, W. Z., Tian, F. A., Ren, Y. J. and Miao, Y. (2018). Research progress on functions of PPR proteins in plant mitochondria and chloroplasts. *J. Fujian Agri. Forestry Univ.* 47, 257–266.
- Wessels, J. G. H., de Vries, O. M. H. D., Asgeirsdottir, S. A., and Schuren, F. (1991). Hydrophobin genes involved in formation of aerial hyphae and fruit bodies in *Schizophyllum*. *Plant Cell*, 3, 793–799. doi: 10.2307/3869273
- Wösten, H. A., Bohlmann, R., Eckerskorn, C., Lottspeich, F., Bölker, M., Kahmann, R., et al. (1996). A novel class of small amphipathic peptides affect aerial hyphal growth and surface hydrophobicity in *Ustilago maydis*. *Embo J.* 15, 4274–4281. doi: 10.1002/j.1460-2075.1996.tb00802.x
- Wösten, H. A. B. and Willey, J. M. (2000). Surface-active proteins enable microbial aerial hyphae to grow into the air. *Microbiology* 146, 767–773. doi: 10.1099/00221287-146-4-767
- Xing, H., Fu, X., Yang, C., Tang, X., Guo, L., Li, C., et al. (2018). Genome-wide investigation of pentatricopeptide repeat gene family in poplar and their expression analysis in response to biotic and abiotic stresses. *Sci. Rep.* 8:2817. doi: 10.1038/s41598-018-21269-1
- Xu, J. R., Staiger, C., and Hamer, J. E. (1998). Inactivation of the mitogen-activated protein kinase mps1 from the rice blast fungus prevents. *Proc. Nat. Acad. Sci. U S A* 95, 12713–12718.
- Xu, F., Song, Y. L., Zhou, Y. L., Zhang, H., Wang, J. M., Li, Y. H., et al. (2016). Occurrence dynamics and characteristics of fusarium root and crown rot of wheat in henan province during 2013–2016. *Plant Prot.* 42, 126–132. doi: 10.3969/j.issn.0529-1542.2016.06.023
- Xu, F., Song, Y. L., Yang, G. Q., Wang, J. M., Liu, L. L., Li, Y. H., et al. (2015). First report of *Fusarium pseudograminearum* from wheat heads with Fusarium head blight in north china plain. *Plant Dis.* 99, 156–156. doi: 10.1094/PDIS-05-14-0543-PDN
- Yago, J. I., Lin, C. H., and Chung, K. R. (2011). The SLT2 mitogen-activated protein kinase-mediated signaling pathway governs conidiation, morphogenesis, fungal virulence and production of toxin and melanin in the tangerine pathotype of *Alternaria alternata*. *Mol. Plant Pathol.* 12, 653–665. doi: 10.1111/j.1364-3703.2010.00701.x
- Yan, J. J., Zhang, Q. X., and Yin, P. (2018). RNA editing machinery in plant organelles. *Sci. China Life Sci.* 61, 162–169. doi: 10.1007/s11427-017-9170-3
- Yanagisawa, S., Kikuma, T., and Kitamoto, K. (2013). Functional analysis of Aogat1 and detection of the Cvt pathway in *Aspergillus oryzae*. *FEMS Microbiol. Lett.* 338, 168–176. doi: 10.1111/1574-6968.12047
- Yang, Y., He, X. L., Hu, Y. F., Hou, Y., Niu, Y. J., Dai, J. L., et al. (2015). Resistance of wheat cultivars in Huang-Huai region of China to crown rot caused by *Fusarium pseudograminearum*. *J. Triticeae Crops* 35, 339–345.
- Zehrmann, A., Verbitskiy, D., HãRtel, B., Brennicke, A., and Takenaka, M. (2011). PPR proteins network as site-specific RNA editing factors in plant organelles. *RNA Biol.* 8, 67–70. doi: 10.4161/rna.8.1.14298
- Zhang, Y. S., Wang, L. M., Liang, S., Zhang, P., Kang, R., Zhang, M., et al. (2020). FpDep1, a component of Rpd3L histone deacetylase complex, is important for vegetative development, ROS accumulation, and pathogenesis in *Fusarium pseudograminearum*. *Fungal Genet. Biol.* 135:103299. doi: 10.1016/j.fgb.2019.103299
- Zhang, J. Y., Sun, J. S., Duan, A. W., Wang, J. L., Shen, X. J., Liu, X. F., et al. (2007). Effects of different planting patterns on water use and yield performance of winter wheat in the Huang-Huai-Hai plain of China. *Agri. Water Manage.* 92, 41–47. doi: 10.1016/j.agwat.2007.04.007
- Zhou, H., He, X., Wang, S., Ma, Q., Sun, B., Ding, S., et al. (2019). Diversity of the Fusarium pathogens associated with crown rot in the Huanghuai wheat growing region of china. *Environ. Microbiol.* 21, 2740–2754. doi: 10.1111/1462-2920.14602
- Zhou, H., Yang, Y., Niu, Y., Yuan, H., and Li, H. (2014). Occurrence and control methods of crown rot of wheat. *J. Henan Agri. Sci.* 43, 114–117. doi: 10.3969/j.issn.1004-3268.2014.05.026

Conflict of Interest: The authors declare that the research was conducted in the absence of any commercial or financial relationships that could be construed as a potential conflict of interest.

Copyright © 2021 Wang, Xie, Zhang, Kang, Zhang, Wang, Li, Chen, Yuan, Ding, Liang and Li. This is an open-access article distributed under the terms of the Creative Commons Attribution License (CC BY). The use, distribution or reproduction in other forums is permitted, provided the original author(s) and the copyright owner(s) are credited and that the original publication in this journal is cited, in accordance with accepted academic practice. No use, distribution or reproduction is permitted which does not comply with these terms.